NUREG/CR-6687
ANL-00/21

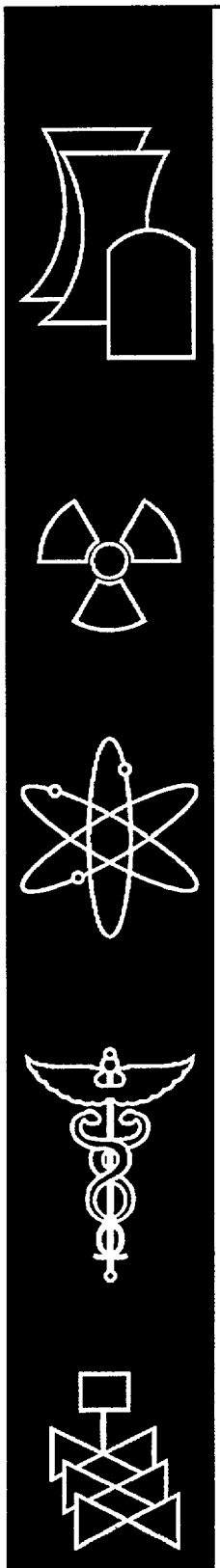

Irradiation-Assisted Stress Corrosion Cracking of Model Austenitic Stainless Steel Alloys

Argonne National Laboratory

U.S. Nuclear Regulatory Commission
Office of Nuclear Regulatory Research
Washington, DC 20555-0001

AVAILABILITY OF REFERENCE MATERIALS IN NRC PUBLICATIONS

NRC Reference Material

As of November 1999, you may electronically access NUREG-series publications and other NRC records at NRC's Public Electronic Reading Room at www.nrc.gov/NRC/ADAMS/index.html.
Publicly released records include, to name a few, NUREG-series publications; *Federal Register* notices; applicant, licensee, and vendor documents and correspondence; NRC correspondence and internal memoranda; bulletins and information notices; inspection and investigative reports; licensee event reports; and Commission papers and their attachments.

NRC publications in the NUREG series, NRC regulations, and *Title 10, Energy*, in the Code of *Federal Regulations* may also be purchased from one of these two sources.

1. The Superintendent of Documents
   U.S. Government Printing Office
   P. O. Box 37082
   Washington, DC 20402–9328
   www.access.gpo.gov/su_docs
   202–512–1800
2. The National Technical Information Service
   Springfield, VA 22161–0002
   www.ntis.gov
   1–800–533–6847 or, locally, 703–805–6000

A single copy of each NRC draft report for comment is available free, to the extent of supply, upon written request as follows:

Address: Office of the Chief Information Officer,
Reproduction and Distribution
Services Section
U.S. Nuclear Regulatory Commission
Washington, DC 20555-0001
E-mail: DISTRIBUTION@nrc.gov
Facsimile: 301–415–2289

Some publications in the NUREG series that are posted at NRC's Web site address www.nrc.gov/NRC/NUREGS/indexnum.html are updated periodically and may differ from the last printed version. Although references to material found on a Web site bear the date the material was accessed, the material available on the date cited may subsequently be removed from the site.

Non-NRC Reference Material

Documents available from public and special technical libraries include all open literature items, such as books, journal articles, and transactions, *Federal Register* notices, Federal and State legislation, and congressional reports. Such documents as theses, dissertations, foreign reports and translations, and non-NRC conference proceedings may be purchased from their sponsoring organization.

Copies of industry codes and standards used in a substantive manner in the NRC regulatory process are maintained at—

The NRC Technical Library
Two White Flint North
11545 Rockville Pike
Rockville, MD 20852–2738

These standards are available in the library for reference use by the public. Codes and standards are usually copyrighted and may be purchased from the originating organization or, if they are American National Standards, from—

American National Standards Institute
11 West 42nd Street
New York, NY 10036–8002
www.ansi.org
212–642–4900

The NUREG series comprises (1) technical and administrative reports and books prepared by the staff (NUREG–XXXX) or agency contractors (NUREG/CR–XXXX), (2) proceedings of conferences (NUREG/CP–XXXX), (3) reports resulting from international agreements (NUREG/IA–XXXX), (4) brochures (NUREG/BR–XXXX), and (5) compilations of legal decisions and orders of the Commission and Atomic and Safety Licensing Boards and of Directors' decisions under Section 2.206 of NRC's regulations (NUREG–0750).

NUREG/CR-6687
ANL-00/21

Irradiation-Assisted Stress Corrosion Cracking of Model Austenitic Stainless Steel Alloys

Manuscript Completed: May 2000
Date Published: October 2000

Prepared by
H. M. Chung, W. E. Ruther,
R. V. Strain, W. J. Shack

Argonne National Laboratory
9700 South Cass Avenue
Argonne, IL 60439

M. McNeil, NRC Project Manager

Prepared for
Division of Engineering Technology
Office of Nuclear Regulatory Research
U.S. Nuclear Regulatory Commission
Washington, DC 20555-0001
NRC Job Code W6610

Irradiation-Assisted Stress Corrosion Cracking of Model Austenitic Stainless Steel Alloys

by
H. M. Chung, W. E. Ruther, R. V. Strain, and W. J. Shack

Abstract

This report summarizes work performed at Argonne National Laboratory on irradiation-assisted stress corrosion cracking (IASCC) of model austenitic stainless steels (SSs) that were irradiated in the Halden boiling heavy water reactor in simulation of the neutronic and environmental conditions of boiling water reactor (BWR) core internal components. Slow-strain-rate tensile tests in simulated BWR water were conducted on model austenitic stainless steel alloys that were irradiated at 289°C in helium to ≈0.3 x 10^{21} n·cm^{-2} and ≈0.9 x 10^{21} n·cm^{-2} (E > 1 MeV). Fractographic analysis by scanning electron microscopy was conducted to determine susceptibility to irradiation-assisted stress corrosion cracking as manifested by the degree of intergranular and transgranular stress corrosion cracking (IGSCC and TGSCC) fracture surface morphology. As fluence was increased from ≈0.3 x 10^{21} n·cm^{-2} to ≈0.9 x 10^{21} n·cm^{-2}, IGSCC fracture surfaces emerged in many alloys, usually in the middle of and surrounded by TGSCC fracture surfaces. Alloy-to-alloy variations in susceptibility to TGSCC and IGSCC were significant at ≈0.9 x 10^{21} n·cm^{-2}. Susceptibility to TGSCC and IGSCC was influenced by more than one alloying and impurity element in a complex manner. Results from this study indicate that for commercial heats of Types 304 and 304L SS, a high concentration of S is detrimental and that a sufficiently low concentration of S is a necessary condition for good resistance to IASCC. A laboratory alloy containing a high concentration of Cr exhibited excellent resistance to TGSCC and IGSCC, despite a high S content, indicating that Cr atoms in high concentration play a major role in suppressing susceptibility to IASCC under BWR conditions. Yield strength of the model alloys, measured in BWR-like water at 289°C, was nearly constant at ≈200 MPa in the unirradiated state and was more or less independent of Si concentration. However, as the alloys were irradiated, the degree of increase in yield strength was significantly lower for alloys that contain >0.9 wt.% Si than for alloys that contain <0.8 wt.% Si, indicating that the nature of irradiation-induced hardening centers and the degree of irradiation hardening is significantly influenced by the Si content of the alloy. Similar influence was not observed for C and N. Results also indicate that a Si content between ≈0.8 and ≈1.5 wt.% is beneficial in delaying the onset of or suppressing the susceptibility to IASCC. Although susceptibility to TGSCC and IGSCC was insignificant and the fracture surface morphology was mostly ductile, some alloys exhibited very low uniform elongation and poor work-hardening capability in water after irradiation to ≈0.9 x 10^{21} n·cm^{-2}. Such alloys contained unusually high concentrations of O or unusually low concentrations of Si or both. To better understand such behavior, usually indicative of severe susceptibility to dislocation channeling or other forms of localized deformation, a systematic microstructural investigation by transmission and scanning electron microscopies is desirable.

Contents

Figures

Tables

Executive Summary

This report summarizes experimental work performed at Argonne National Laboratory on irradiation-assisted stress corrosion cracking of model austenitic stainless steels that were irradiated in the Halden Boiling Heavy Water Reactor in simulation of irradiation-induced degradation of boiling water reactor (BWR) core internal components. Slow-strain-rate tensile tests in simulated BWR water were conducted on twenty-three model austenitic stainless steel alloys that were irradiated at 288°C in helium in the Halden reactor to a fluence of $\approx 0.9 \times 10^{21}$ n·cm^{-2} (E > 1 MeV). A similar investigation of the behavior of sixteen alloys irradiated to a fluence of $\approx 0.3 \times 10^{21}$ n·cm^{-2} (E > 1 MeV) has been reported previously. Fractographic analysis by scanning electron microscopy was conducted to determine the susceptibility to irradiation-assisted stress corrosion cracking as manifested by the degree of intergranular and transgranular fracture surface morphology.

At $\approx 0.3 \times 10^{21}$ n·cm^{-2} (E > 1 MeV), many alloys were susceptible to transgranular stress corrosion cracking, but only one alloy of Type 316L stainless steel that contains a very low concentration of Si (0.024 wt.% Si) was susceptible to intergranular stress corrosion cracking. Alloy-to-alloy variations in susceptibility to transgranular stress corrosion cracking were significant at $\approx 0.3 \times 10^{21}$ n·cm^{-2}. As fluence was increased from $\approx 0.3 \times 10^{21}$ n·cm^{-2} to $\approx 0.9 \times 10^{21}$ n·cm^{-2}, intergranular fracture surfaces emerged in many alloys, usually in the middle of and surrounded by transgranular fracture surfaces. This indicates that for many alloys high susceptibility to transgranular stress corrosion cracking is a precursor to susceptibility to intergranular stress corrosion cracking at a higher fluence. Alloy-to-alloy variations in susceptibility to transgranular and intergranular stress corrosion cracking were significant at $\approx 0.9 \times 10^{21}$ n·cm^{-2}. Susceptibility to transgranular and intergranular stress corrosion cracking was influenced by more than one alloying and impurity element in a complex manner.

In unirradiated state and at the relatively low fluence level of $\approx 0.3 \times 10^{21}$ n·cm^{-2}, commercial and laboratory heats of Types 304, 304L, and 348 stainless steel that contain relatively high concentrations of S (>0.009 wt.% S, 15-18.50 wt.% Cr) exhibited significant susceptibility to transgranular stress corrosion cracking, whereas alloys that contain relatively low concentrations of S (<0.005 wt.% S) exhibited good resistance to transgranular stress corrosion cracking. At $\approx 0.9 \times 10^{21}$ n·cm^{-2}, commercial heats of Types 304 and 316 stainless steel that contain low concentrations of S exhibited high resistance to transgranular and intergranular stress corrosion cracking and high levels of uniform and total elongation, whereas a commercial heat of Type 304 stainless steel that contained a relatively high concentration of S exhibited poor resistance to transgranular and intergranular stress corrosion cracking and low levels of uniform and total elongation. These observations indicate that for commercial heats of Types 304 and 304L stainless steel, a high concentration of S (>0.009 wt.% S) is significantly detrimental and that a sufficiently low concentration of S is a necessary condition for good resistance to IASCC. At $\approx 0.9 \times 10^{21}$ n·cm^{-2}, a laboratory alloy that contains a high concentration of Cr (≈21 wt.%) exhibited excellent resistance to transgranular and intergranular stress corrosion cracking, in spite of a high S content (≈0.028 wt.% S), whereas heats with <17.5 wt.% Cr exhibited significant susceptibility to transgranular plus intergranular stress corrosion cracking. This finding indicates that Cr atoms in high concentration play a major role in suppressing susceptibility to irradiation-assisted stress corrosion cracking under BWR conditions.

Yield strength of unirradiated model alloys, measured in BWR-like water at 289°C, was nearly constant at ≈200 MPa and was more or less independent of Si concentration. However, as the alloys were irradiated to ≈0.3 x 10^{21} n·cm^{-2} and ≈0.9 x 10^{21} n·cm^{-2}, the degree of increase in yield strength was significantly lower for alloys that contain >0.9 wt.% Si than for alloys that contain <0.8 wt.% Si. This observation indicates that the nature of irradiation-induced hardening centers and the degree of irradiation hardening is significantly influenced by the Si content of the alloy. A similar influence was not observed for C and N. Among laboratory heats of Types 304 and 304L stainless steel, alloys that contain <0.67 wt.% Si exhibited significant susceptibility to intergranular stress corrosion cracking, whereas heats with 0.8-1.5 wt.% Si exhibited negligible susceptibility to intergranular stress corrosion cracking. However, an alloy with ≈1.9 wt.% Si exhibited some degree of susceptibility to intergranular stress corrosion cracking. These observations indicate that a Si content between ≈0.8 and ≈1.5 wt.% is beneficial in delaying the onset of, or suppressing, susceptibility to irradiation-assisted stress corrosion cracking. Consistent with the effects of S, Cr, and Si, an alloy that contains unusually low concentrations of Cr and Si and unusually high concentrations of S and O exhibited the worst susceptibility to IASCC at ≈0.9 x 10^{21} n·cm^{-2}.

Although susceptibility to transgranular and intergranular stress corrosion cracking was insignificant and the fracture surface morphology was mostly ductile, some alloys exhibited very low uniform elongation and poor work-hardening capability in water after irradiation to ≈0.9 x 10^{21} n·cm^{-2}. Such alloys contained unusually high concentrations of O or unusually low concentrations of Si or both. To better understand such behavior, usually indicative of severe susceptibility to dislocation channeling or other forms of localized deformation, a systematic microstructural investigation by transmission and scanning electron microscopies will be needed. A few alloys that contain unusually high concentrations of O exhibited either high susceptibility to intergranular stress corrosion cracking or poor work-hardening capability. Therefore, it appears that a high concentration of O is also detrimental.

Acknowledgments

The authors sincerely thank T. M. Karlsen, OECD Halden Reactor Project, Halden, Norway, for performing specimen irradiation in the Halden reactor; D. R. Perkins and R. W. Clark for conducting the slow-strain-rate tensile tests on the irradiated specimens. The authors are also grateful to M. B. McNeil for many helpful discussions.

1 Introduction

In recent years, failures of reactor core internal components have increased after accumulating a fluence >0.5 x 10^{21} n·cm^{-2} (E >1 MeV), or ≈0.7 dpa, in boiling water reactors (BWRs), and at approximately one order of magnitude higher fluences in some pressurized water reactors (PWRs). The general pattern of the observed failures indicates that as nuclear plants age and neutron fluence increases, various nonsensitized austenitic stainless steels (SSs) become susceptible to intergranular failure. Some components are known to have cracked under minimal applied stress. Although most failed components can be replaced, some safety-significant structural components (e.g., the BWR top guide, shroud, and core plate) would be very costly or impractical to replace. Therefore, the structural integrity of these components at high fluence has been a subject of concern, and extensive research has been conducted to provide an understanding of this type of degradation, which is commonly known as irradiation-assisted stress corrosion cracking (IASCC).

Irradiation profoundly affects both local coolant-water chemistry and component microstructure. The primary effects of irradiation on materials include alteration of local microchemistry, microstructure, and mechanical properties of the core internal components, which are usually fabricated from American Society of Testing and Materials (ASTM) Types 304, 316, or 348 SS. Irradiation produces defects and defect clusters in grain matrices, alters the dislocation and dislocation loop structures, and produces defect-impurity and defect-cluster-impurity complexes, leading to radiation-induced hardening and, in many cases, flow localization via dislocation channeling. Irradiation also leads to changes in the stability of second-phase precipitates and the local alloy chemistry near grain boundaries, precipitates, and defect clusters. Grain-boundary microchemistry that significantly differs from bulk composition can be produced in association with not only radiation-induced segregation but also thermally driven equilibrium and nonequilibrium segregation of alloying and impurity elements.

For many years, irradiation-induced grain-boundary depletion of Cr has been considered the primary metallurgical process that causes IASCC. One of the most important factors that has been considered by many investigators to support the Cr-depletion mechanism is the similarity in dependence on water chemistry (i.e., oxidizing potential) of intergranular stress corrosion cracking (IGSCC) of both nonirradiated thermally sensitized material and IASCC of BWR-irradiated solution-annealed material.[1-3] However, contrary to expectations based on the Cr-depletion mechanism, cracking incidents of control rod cladding and baffle plate bolts have been reported at numerous PWRs (i.e., under nonoxidizing potential). Also, the susceptibility of PWR-irradiated components to IASCC has been shown clearly by expanding-mandrel[4] and slow-strain-rate tensile (SSRT)[5] tests in PWR water[4] or PWR-simulated water,[5] although PWR water chemistry falls well within the range of protective electrochemical potential (ECP).[1-3]

Other investigators have implicated radiation-induced segregation of ASTM-specified impurities, such as Si, P, and S, as the primary process that causes IASCC.[4,6,7] The superior resistance of one heat of Type 348 SS that is especially low in C, Si, P, and S seemed to provide support for this process,[4] and the same rationale was extended to Type 304 SS. However, in direct contradiction, several investigators recently reported that resistance of high-purity (HP) heats (low in C, Si, S, and P) of Type 304 SS is no better than that of

commercial–purity (CP) Type 304 SSs.[8-14] Therefore, the role of grain–boundary segregation of Si, P, and S appears to be not well established.

Although C significantly increases the yield strength of irradiated stainless steels, higher C content seems to be either benign or even conducive to lower susceptibility to intergranular cracking of irradiated materials.[14] Deleterious effects of O in steels have been reported by Chung et al.[14] and Cookson et al.[15] Indications of the deleterious effect of grain–boundary segregation of N have been reported for BWR neutron absorber tubes fabricated from high- and commercial-purity heats of Type 304 SS.[14] Similar reports suggest that a higher concentration of N is deleterious, at least under BWR conditions.[6,12,16,17] Indications of the deleterious role of N have also been reported for Types 304L and 316L SSs that contain <0.024 wt.% C and have been irradiated in BWRs or test reactors at 240–300°C.[11] Kasahara et al.[16] also reported that higher N in Type 316L increased the susceptibility to IASCC, indicating that Type 316LN is a susceptible material. This observation is consistent with the behavior of 316NG SSs reported by Jacobs et al.[6] and Jenssen and Ljungberg.[17] In contrast to these observations, 316NG SSs irradiated at ≈50°C has been reported to be resistant to intergranular failure at ≈288°C in water that contained ≈32 ppm dissolved oxygen (DO).[11] Therefore, the role of N appears to be neither clear nor convincing.

In general, IASCC is characterized by strong heat-to-heat variation in susceptibility, in addition to strong dependence on irradiation condition, material type, and grade, even among materials of virtually identical chemical composition. This situation indicates that the traditional interpretation based on the role of grain-boundary Cr depletion cannot completely explain the mechanism of IASCC. Thus, although most investigators believe that significant grain-boundary Cr depletion plays an important role, other important processes that could be associated with other minor impurity elements may have been overlooked.[14] Therefore, we have initiated a new irradiation testing program to systematically investigate the effects of alloying and impurity elements (Cr, Ni, Si, P, S, Mn, C, and N) on the susceptibility of austenitic SSs to IASCC at several fluence levels. Construction of the test matrix was based on the method of Taguchi,[18] and susceptibility to IASCC was determined by SSRT testing of the specimens irradiated in BWR-simulated water and post-testing fractographic examination by scanning electron microscopy (SEM). This report summarizes the results obtained from 16 model austenitic stainless steel alloys that were irradiated at 288°C in He in the Halden reactor to a fluence of $\approx 0.3 \times 10^{21}$ n·cm^{-2} (E > 1 MeV) and 23 alloys irradiated to a fluence of $\approx 0.9 \times 10^{21}$ n·cm^{-2} (E > 1 MeV).

2 Test Matrix and Specimen Fabrication

2.1 Construction of Test Matrix

The irradiation test matrix was constructed according to the method of Taguchi, which is described in Ref. 18. The base matrix followed Taguchi's standard orthogonal array L_{18} (2^1 x 3^7) which is an optimized matrix designed to determine systematically the effects of seven variables (i.e., bulk material concentrations of Cr, Si, P, S, Mn, C, and N) at three concentration levels, and one variable (Ni concentration) at two levels. A possible synergistic interaction was assumed only between Ni and Si. Compositions assigned to the three levels of the seven alloying and impurity elements and two levels of Ni are given in Table 1. The basic test matrix, optimized on the basis of Taguchi's orthogonal array L_{18} (2^1 x 3^7), is given in Table 2.

Table 1. Compositions assigned to medium, high, and low levels of alloying and impurity elements used to construct Taguchi's L_{18} (2^1 x 3^7) array

Factor No.	Element Assigned	Composition (in wt.%) Assigned to Level		
		High	Medium	Low
1	Ni	10.000	8.000	–
2	Si	1.400	0.700	0.150
3	P	0.090	0.040	0.020
4	S	0.020	0.006	0.002
5	Mn	2.050	1.200	0.500
6	C	0.090	0.040	0.010
7	N	0.090	0.040	0.010
8	Cr	18.500	17.500	16.000

In addition to the 18 statistically optimized heats given in Table 2, six supplementary heats of commercial- and high-purity (CP and HP) grade Types 304, 316, and 348 SS were included in the test matrix. Compositions of the six supplementary heats are given in Table 3. Of the 24 heats given in Tables 1 and 2, eight (i.e., Heats 1, 3, 9, 10, 12, 16, 19, and 21) were replaced by commercially fabricated and purchased heats. Compositions of major impurities (i.e., Si, P, C, and N) of each of the eight commercial heats matched closely those of each corresponding heat given in Tables 1 and 2. The prefix "C" was added to the identification number of these eight commercial heats (see Table 4).

The remaining 16 heats in Tables 1 and 2 were fabricated in the laboratory. All of the laboratory-fabricated heats were designated with identification numbers that began with "L". To this matrix of 24 heats, three laboratory heats were added to test the effects of the fabrication procedure. Compositions of these three laboratory heats (i.e., Heats L25C3,

L26C19, and L27C21 in Table 4) closely match those of the corresponding commercial heats (Heats C3, C19, and C21), respectively. Elemental compositions of the complete test matrix, comprising 27 model austenitic SSs, is given in Table 4.

Table 2. Basic test matrix optimized according to Taguchi's orthogonal array L_{18} ($2^1 \times 3^7$)

Heat	Composition (in wt.%)							
No.	Ni	Si	P	S	Mn	C	N	Cr
1	10.0	0.70	0.04	0.006	1.20	0.04	0.04	18.5
2	10.0	0.70	0.09	0.020	2.05	0.09	0.09	17.5
3	10.0	0.70	0.02	0.002	0.50	0.01	0.01	16.0
4	10.0	1.40	0.04	0.006	2.05	0.09	0.01	16.0
5	10.0	1.40	0.09	0.020	0.50	0.01	0.04	18.5
6	10.0	1.40	0.02	0.002	1.20	0.04	0.09	17.5
7	10.0	0.15	0.04	0.020	1.20	0.01	0.09	16.0
8	10.0	0.15	0.09	0.006	2.05	0.04	0.01	18.5
9	10.0	0.15	0.02	0.002	0.50	0.09	0.04	17.5
10	8.0	0.70	0.04	0.002	0.50	0.09	0.09	18.5
11	8.0	0.70	0.09	0.006	1.20	0.01	0.01	17.5
12	8.0	0.70	0.02	0.020	2.05	0.04	0.04	16.0
13	8.0	1.40	0.04	0.020	0.50	0.04	0.01	17.5
14	8.0	1.40	0.09	0.002	2.05	0.09	0.04	16.0
15	8.0	1.40	0.02	0.006	1.20	0.01	0.09	18.5
16	8.0	0.15	0.04	0.002	2.05	0.01	0.04	17.5
17	8.0	0.15	0.09	0.006	0.50	0.04	0.09	16.0
18	8.0	0.15	0.02	0.020	1.20	0.09	0.01	18.5

Table 3. Composition (in wt.%) of six supplementary commercial- and high-purity (CP and HP) heats of Types 304, 316, and 348 stainless steels

Heat	SS Type	C	N	Si	P	S	Mn	Cr	Ni	Nb	Mo
19	CP 304	0.04	0.04	0.70	0.04	0.06	1.20	18.5	10.0	-	-
20	HP 304	0.01	0.01	0.15	0.02	0.02	0.50	18.5	10.0	-	-
21	CP 316	0.04	0.04	0.70	0.04	0.06	1.20	16.5	13.5	-	2.20
22	HP 316	0.01	0.01	0.15	0.02	0.02	0.50	16.5	13.5	-	2.20
23	CP 348	0.04	0.04	0.70	0.04	0.06	1.20	17.5	11.5	2.20	-
24	HP 348	0.01	0.01	0.15	0.02	0.02	0.50	17.5	11.5	2.20	-

Table 4. Elemental composition of 27 commercial and laboratory model austenitic stainless steel alloys irradiated in Halden Reactor

ANL	Source	Composition (wt.%)										
ID[a]	Heat ID	Ni	Si	P	S	Mn	C	N	Cr	O	B	Mo or Nb
C1	DAN-70378	8.12	0.50	0.038	0.002	1.00	0.060	0.060	18.11	-	<0.001	-
L2	BPC-4-111	10.50	0.82	0.080	0.034	1.58	0.074	0.102	17.02	0.0066	<0.001	-
C3	PNL-C-1	8.91	0.46	0.019	0.004	1.81	0.016	0.083	18.55	-	<0.001	-
L4	BPC-4-88	10.20	0.94	0.031	0.010	1.75	0.110	0.002	15.80	-	<0.001	-
L5	BPC-4-104	9.66	0.90	0.113	0.028	0.47	0.006	0.033	21.00	-	<0.001	-
L6	BPC-4-127	10.00	1.90	0.020	0.005	1.13	0.096	0.087	17.10	0.0058	<0.001	-
L7	BPC-4-112	10.60	0.18	0.040	0.038	1.02	0.007	0.111	15.40	0.0274	<0.001	-
L8	BPC-4-91	10.20	0.15	0.093	0.010	1.85	0.041	0.001	18.30	-	<0.001	-
C9	PNL-C-6	8.75	0.39	0.013	0.013	1.72	0.062	0.065	18.48	-	<0.001	-
C10	DAN-23381	8.13	0.55	0.033	0.002	1.00	0.060	0.086	18.19	-	<0.001	-
L11	BPC-4-93	8.15	0.47	0.097	0.009	1.02	0.014	0.004	17.40	-	<0.001	-
C12	DAN-23805	8.23	0.47	0.018	0.002	1.00	0.060	0.070	18.43	-	<0.001	-
L13	BPC-4-96	8.18	1.18	0.027	0.022	0.36	0.026	0.001	17.40	-	<0.001	-
L14	BPC-4-129	7.93	1.49	0.080	0.002	1.76	0.107	0.028	15.00	0.0045	<0.001	-
L15	BPC-4-126	8.00	1.82	0.010	0.013	1.07	0.020	0.085	17.80	0.0110	<0.001	-
C16	PNL-SS-14	12.90	0.38	0.014	0.002	1.66	0.020	0.011	16.92	-	<0.001	-
L17	BPC-4-128	8.00	0.66	0.090	0.009	0.48	0.061	0.078	15.30	0.0090	<0.001	-
L18	BPC-4-98	8.13	0.14	0.016	0.033	1.13	0.080	0.001	18.00	-	<0.001	-
C19	DAN-74827	8.08	0.45	0.031	0.003	0.99	0.060	0.070	18.21	-	<0.001	-
L20	BPC-4-101	8.91	0.17	0.010	0.004	0.41	0.002	0.002	18.10	-	<0.001	-
C21[b]	DAN-12455	10.24	0.51	0.034	0.001	1.19	0.060	0.020	16.28	-	<0.001	Mo 2.08
L22[c]	BPC-4-100	13.30	0.24	0.015	0.004	0.40	0.003	0.001	16.10	-	<0.001	Mo 2.04
L23[d]	BPC-4-114	12.04	0.68	0.030	0.047	0.96	0.043	0.092	17.30	0.0093	<0.001	Nb 1.06
L24[e]	BPC-4-105	12.30	0.03	0.007	0.005	0.48	0.031	0.002	16.90	0.0129	<0.001	Nb 1.72
L25C3	BPC-4-133	8.93	0.92	0.020	0.008	1.54	0.019	0.095	17.20	0.0085	0.010	-
L26C19	BPC-4-131	8.09	0.79	0.004	0.002	0.91	0.070	0.089	17.20	0.0080	<0.001	-
L27C21	BPC-4-132	10.30	0.96	0.040	0.002	0.97	0.057	0.019	15.30	0.0058	0.030	Mo 2.01

[a]First letters "C" and "L" denote commercial and laboratory heats, respectively.
[b]Commercial-purity Type 316 SS.
[c]High-purity Type 316 SS.
[d]Commercial-purity Type 348 SS.
[e]High-purity Type 348 SS.

2.2 Fabrication of Test Specimens

Slow-strain-rate tensile specimens were machined from solution-annealed and water-quenched plates or sheets that were fabricated from the 27 model austenitic SS alloys. The geometry of the SSRT specimens, 0.76 mm thick, 57.2 mm long, and 12.7 mm wide (gauge section 19.1 mm long and 3.1 mm wide), is shown in Fig. 1. Gauge lengths and planes of the specimens were parallel to the rolling direction and plane of the sheets, respectively. Subsize compact-tension (1/4TCT) specimens were also irradiated in tandem in the same capsules with the SSRT specimens to determine J-R fracture toughness properties and crack growth rates (CGRs) after irradiation. Together, 96 SSRT and 24 CT specimens were prepared and irradiated in this study. After these specimens were mechanically machined in the shop, no additional heat-treatment was applied to any of the specimens. The machined specimens were degreased in acetone and cleaned ultrasonically in alcohol before encapsulation in Type 304 SS capsules filled with research-grade He for irradiation in the Halden reactor.

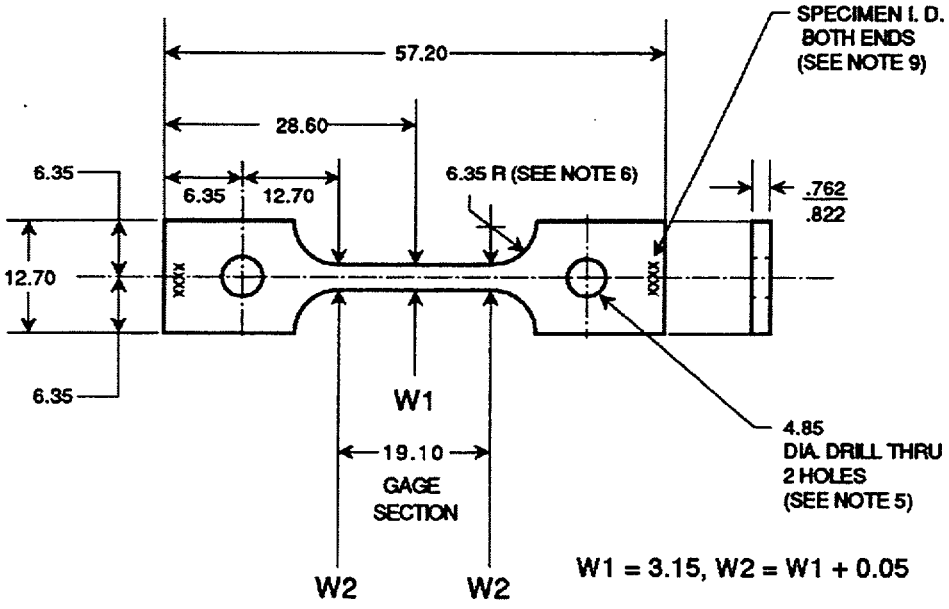

Fig. 1. Geometry of slow-strain-rate tensile specimens; all dimensions in mm

3 Specimen Irradiation

A total of 96 SSRT and 24 CT specimens were encapsulated into six capsules, each capsule containing 16 SSRT and 4 CT specimens. A fixed 0.5-mm gap was allowed between the inner wall of the Type 304 SS capsule and specimen edges. The gap was filled with research-grade He. The gap size of 0.5 mm was selected to maintain specimen temperature at 288°C during irradiation in He. To prevent capsule wall creepdown and possible changes in gap size, spacers in the form of Type 304 SS wires (0.5 mm diameter) were placed between the specimens and the capsule inner wall. Type 304 SS filler bodies were inserted on both sides of the SSRT specimen stack to avoid overheating the thin gauge section. Table 5 shows the specimens categorized according to alloy, fluence level, and postirradiation test type. The six capsules were irradiated in the Halden boiling heavy water reactor starting April 8, 1992. Fast neutron (E > 1MeV) flux during the various irradiation cycles ranged from 1.80×10^{13} n cm^{-2} s^{-1} to 3.31×10^{13} n cm^{-2} s^{-1}. Irradiation history of the six capsules is summarized in Table 6.

Table 5. Summary of specimen number per alloy, irradiation fluence, and postirradiation test type

Specimen	SSRT Test			Uniaxial Constant Load Test			J-R or Crack Growth Rate Test		
ID	high[a]	medium[a]	low[a]	high	medium	low	high	medium	low
C1	1	1	1						
L2	1	1					1	1	
C3	1	1	1				1	1	1
L4	1	1	1						
L5	1	1	1				1		
L6	1	1							
L7	1	1							
L8	1	1	1						
C9	1	1	1						
C10	1	1	1						
L11	1	1	1						
C12	1	1	1						
L13	1	1	1						
L14	1	1					1		
L15	1	1							
C16	1	1	1				1	1	
L17	1	1							
L18	1	1	1				1	1	
C19	5	1	1	4	4		1	1	1
L20	5	1	1	4	4		1	1	1
C21	1	1	1				1	1	1
L22	1	1	1				1	1	
L23	1	1					1		
L24	1	1					1		
L25C3	3								
L26C19	3								
L27C21	2								

[a]Fluence level in 10^{21} n cm^{-2} (E > 1 MeV): high ≈ 2.5, medium ≈ 0.9, and low ≈ 0.3.

Table 6. Summary of discharge fluence of model austenitic stainless steel alloys irradiated in Halden Boiling Heavy Water Reactor

Capsule ID	Fluence Level	Target Fluence[a] (10^{21} n cm^{-2})	Irradiation Cycles	Discharge Date	Discharge Fluence[a] (10^{21} n cm^{-2})
1	medium	1.0	IFA 530-3 to -6; D-07-004-2	Nov. 96	0.9
4	low	0.4	IFA 530-3	Oct. 92	0.3
5	high	2.5	IFA 530-4 to -6; D-07-004-1 to -3	Nov. 99	2.0
6	high	2.5	IFA 530-4 to -5; D-07-004-1 to -3	Nov. 99	2.0
7	medium	1.0	IFA 530-4 and -6; D-07-004-1	May 96	0.9
8	high	2.5	IFA 530-5 to -6; D-07-004-1 to -3	Nov. 99	2.0

[a]For neutron energy E >1 MeV

4 SSRT Test and SEM Fractography on Medium-Fluence Specimens

Slow-strain-rate tensile tests and fractographic analysis by SEM have been completed for the 16 alloys that were irradiated to a fluence of ≈0.3 x 10^{21} n·cm^{-2} (E > 1 MeV) at ≈288°C in an He environment in the Halden reactor. Tests were also completed on 23 medium-fluence alloy specimens irradiated to ≈0.9 x 10^{21} n·cm^{-2} (E > 1 MeV). In addition to the irradiated specimens, unirradiated control specimens were tested under the same conditions. All SSRT tests were conducted at 289°C in simulated BWR water that contained ≈8 ppm DO.

Conductivity and pH of the water were kept at ≈0.07-0.10 and 6.3-6.8, respectively. Strain rate was held constant at 1.65 x 10^{-7} s^{-1}. Electrochemical potential was measured on the effluent side at regular intervals.

Comprehensive results of SSRT testing and fractographic analysis of the unirradiated control specimens and specimens irradiated to low fluence of ≈0.3 x 10^{21} n·cm^{-2} (E > 1 MeV) were reported previously.[19] For comparison with similar results obtained from specimens irradiated to medium fluence of ≈0.9 x 10^{21} n·cm^{-2} (E > 1 MeV) given in this report, results obtained for zero and low fluence are summarized in Tables 7-10. Feedwater chemistry (i.e., DO, ECP, conductivity, and pH) and results from SSRT testing (i.e., 0.2%-offset yield strength, maximum strength, uniform plastic strain, and total plastic strain) are summarized in Tables 7 and 9, respectively, for nonirradiated control specimens and specimens irradiated to ≈0.3 x 10^{21} n·cm^{-2} (E > 1 MeV). Also shown in these tables are results of SEM fractographic analysis of the failure mode (i.e., ductile, intergranular, and transgranular fracture surface morphology) of the specimens. In Table 8, the results of SSRT and SEM fractographic analysis (percent IGSCC, percent TGSCC, and combined percent IGSCC+TGSCC) are correlated with compositional characteristics of the unirradiated specimens. Similar correlations for alloys irradiated to ≈0.3 x 10^{21} n·cm^{-2} (E > 1 MeV) are given in Table 10.

4.1 Results of SSRT Tests and SEM Fractography

Results of SSRT tests and SEM fractography conducted on medium-fluence specimens irradiated to ≈0.9 x 10^{21} n cm^{-2} (E > 1 MeV) are summarized in Table 11. The results are correlated with the compositional characteristics of the alloys in Table 12.

The results obtained from the SSRT tests and SEM fractography of the medium-fluence specimens, i.e., yield strength, ultimate tensile strength, uniform elongation, total elongation, percent TGSCC, percent IGSCC, and percent TGSCC+IGSCC, are plotted for each alloy in Figs. 2-8, respectively. When compared with the properties of the unirradiated and low-fluence specimens, the effects of the increased fluence on yield strength, ultimate tensile strength, uniform elongation, total elongation, and fracture behavior of the medium-fluence specimens were significant. For example, the effects of fluence and test environment (i.e., air vs. water) on load elongation behavior are shown in Fig. 9 for Heat C19, a commercially purchased heat of Type 304 SS. For the commercial alloy, a significant effect of fluence on load-elongation behavior in water is evident as fluence increases from 0 to ≈0.3 x 10^{21} n cm^{-2} and ≈0.9 x 10^{21} n cm^{-2}. A similar effect of fluence was significantly more pronounced for most laboratory alloys than for commercial alloys.

Table 7. Results of SSRT[a] test and SEM fractography for nonirradiated control specimens of model austenitic stainless steel alloys.

Alloy and Specimen Ident. No.	SSRT No.	Feedwater Chemistry				SSRT Parameters				Fracture Behavior		
		Oxygen Conc. (ppm)	Average ECP (mV SHE)	Cond. at 25°C ($\mu S \cdot cm^{-1}$)	pH at 25°C	Yield Stress (MPa)	Max. Stress (MPa)	Uniform Elong. (%)	Total Elong. (%)	TGSCC (%)	IGSCC (%)	TGSCC+ IGSCC (%)
L23-4	CHR–1	8.6	+228	0.07	6.65	332	480	15.6	17.0	15	0	15
L7-4	CHR-2	8.0	+217	0.07	7.37	195	370	2.5	5.2	20	0	20
L7-B1	CHR-7		tested in air			282	676	42.3	43.9	0	0	0
L14-4	CHR-3	8.6	+208	0.07	7.37	240	474	41.8	44.2	0	0	0
L17-4	CHR-4	7.5	+262	0.06	7.09	189	412	11.6	13.3	60	0	60
L17-B1	CHR-19	7.8	+166	0.08	6.71	184	447	30.1	31.2	8	0	8
L6-4	CHR-5	7.9	+256	0.08	6.85	227	515	43.0	44.5	0	0	0
L27-4	CHR-6	9.3	+247	0.08	6.96	298	483	20.6	22.9	0	0	0
L26-4	CHR-8	9.4	+223	0.07	6.65	184	506	38.2	40.2	0	0	0
L2-4	CHR-9	8.6	+292	0.06	6.55	193	348	6.6	7.8	57	0	57
L25-4	CHR-10	8.2	+239	0.06	6.42	184	458	25.5	27.0	0	0	0
L15-4	CHR-11	8.2	+195	0.06	6.32	218	512	36.7	37.9	0	0	0
L24-4	CHR-12	8.4	+200	0.07	6.20	352	461	10.4	12.3	10	0	10
C1-15	CHR-13	8.1	+187	0.07	6.33	179	498	49.4	51.7	0	0	0
C19-B1	CHR-14	8.8	+179	0.08	6.29	178	501	47.4	49.2	0	0	0
C9-B1	CHR-15	8.5	+166	0.07	6.83	178	408	17.4	19.4	32	0	32
C12-B1	CHR-16	8.5	+124	0.07	6.18	182	511	46.0	47.6	0	0	0
C10-B1	CHR-17	9.2	+145	0.07	6.26	174	478	30.6	35.1	0	0	0
C21-9	CHR-18	9.2	+187	0.07	6.41	277	455	48.9	59.5	0	0	0

[a]Tested at 289°C at a strain rate of 1.65×10^{-7} s^{-1} in simulated BWR water containing ≈8 ppm DO.

Table 8. Compositionional characteristics (composition in wt.%) of nonirradiated control specimens of model austenitic stainless steel alloys correlated with results of SSRT test[a] and SEM fractography (HP = high purity, CP = commercial purity).

Alloy ID	Ni	Si	P	S	Mn	C	N	Cr	Mo/Nb	O (wppm)	Remark[b]	YS (MPa)	UTS (MPa)	UE (%)	TE (%)	TGSCC (%)	IGSCC (%)	TG+IGSCC (%)
L23	12.04	0.68	0.030	0.047	0.96	0.043	0.092	17.30	Nb 1.06	93	CP 348	332	480	15.6	17.0	15	0	15
L7	10.60	0.18	0.040	0.038	1.02	0.007	0.111	15.40	-	274	High N, O; Low Si, C	195	370	2.5	5.2	20	0	20
L14	7.93	1.49	0.080	0.002	1.76	0.107	0.028	15.00	-	45	High Si, P, C; Low S	240	474	41.8	44.2	0	0	0
L17	8.00	0.66	0.090	0.009	0.48	0.061	0.078	15.30	-	90	High P; Low Cr, Mn, S	189	412	11.6	13.3	60	0	60
L17	8.00	0.66	0.090	0.009	0.48	0.061	0.078	15.30	-	90	High P; Low Cr, Mn, S	184	447	30.1	31.2	8	0	8
L6	10.00	1.90	0.020	0.005	1.13	0.096	0.087	17.10	-	58	High Si, C, Cr; Low S	227	515	43.0	44.5	0	0	0
L27	10.30	0.96	0.040	0.002	0.97	0.057	0.019	15.30	Mo 2.01	-	CP 316 ; high B (0.030)	298	483	20.6	22.9	0	0	0
L26	8.09	0.79	0.004	0.002	0.91	0.070	0.089	17.20	-	80	Low P, S	184	506	38.2	40.2	0	0	0
L2	10.50	0.82	0.080	0.034	1.58	0.074	0.102	17.02	-	66	High P, S, Mn, N	193	348	6.6	7.8	57	0	57
L25	8.93	0.92	0.020	0.008	1.54	0.019	0.095	17.20	-	85	high B (0.010)	184	458	25.5	27.0	0	0	0
L15	8.00	1.82	0.010	0.013	1.07	0.020	0.085	17.80	-	110	High N; Low C	218	512	36.7	37.9	0	0	0
L24	12.30	0.03	0.007	0.005	0.48	0.031	0.002	16.90	Nb 1.72	-	HP 348; Low Si, N	352	461	10.4	12.3	10	0	10
C1	8.12	0.50	0.038	0.002	1.00	0.060	0.060	18.11	-	-	Low S, CP 304	179	498	49.4	51.7	0	0	0
C19	8.08	0.45	0.031	0.003	0.99	0.060	0.070	18.21	-	-	Low Si, S, CP 304	178	501	47.4	49.2	0	0	0
C9	8.75	0.39	0.013	0.013	1.72	0.062	0.065	18.48	-	-	Low Si, High Mn	178	408	17.4	19.4	32	0	32
C12	8.23	0.47	0.018	0.002	1.00	0.060	0.070	18.43	-	-	Low Si, S, P	182	511	46.0	47.6	0	0	0
C10	8.13	0.55	0.033	0.002	1.00	0.060	0.086	18.19	-	-	Low S, high N	174	478	30.6	35.1	0	0	0
C21	10.24	0.51	0.034	0.001	1.19	0.060	0.020	16.28	Mo 2.08	-	CP 316; low B (0.001)	277	455	48.9	59.5	0	0	0

[a]Test at 289°C at a strain rate of 1.65×10^{-7} s^{-1} in simulated BWR water.

Table 9. Results of SSRT[a] test and SEM fractography for model austenitic stainless steels irradiated in helium at 289°C to fluence of ≈0.3 x 10^{21} n·cm^{-2} (E > 1 MeV).

Alloy and Specimen Ident. No.	SSRT No.	Feedwater Chemistry: Oxygen Conc. (ppm)	Feedwater Chemistry: Average ECP (mV SHE)	Feedwater Chemistry: Cond. at 25°C (µS·cm^{-1})	Feedwater Chemistry: pH at 25°C	SSRT Parameters: Yield Stress (MPa)	SSRT Parameters: Max. Stress (MPa)	SSRT Parameters: Uniform Elongation (%)	SSRT Parameters: Total Elongation (%)	Fracture Behavior: TGSCC (%)	Fracture Behavior: IGSCC (%)	Fracture Behavior: TGSCC + IGSCC (%)
C1-1	HR-1	8.3	+184	0.07	7.03	490	680	13.4	16.6	4	0	4
L5-1	HR-2	9.7	+208	0.07	6.89	513	539	29.5	32.7	2	2	4
L22-1	HR-3	8.0	+236	0.07	6.80	360	596	6.6	9.4	50	15	65
C3-1	HR-4	8.7	+161	0.07	6.68	338	491	27.7	31.6	5	0	5
C16-1	HR-5	8.3	+204	0.08	6.74	370	527	17.6	20.6	2	0	2
L4-1	HR-6	9.0	+202	0.08	6.70	367	542	19.7	22.3	46	0	46
L18-1	HR-7	9.0	+203	0.08	6.33	503	572	6.3	8.8	54	0	54
C10-1	HR-8	8.2	+174	0.07	6.35	523	640	17.4	18.9	6	0	6
C21-1	HR-9	8.1	+149	0.08	6.49	480	620	15.9	19.4	4	0	4
L11-1	HR-10	9.0	+157	0.08	6.17	487	599	2.3	3.8	62	0	62
L13-1	HR-11	8.7	+164	0.08	6.17	248	461	22.1	24.8	8	0	8
L20-1	HR-12	8.4	+174	0.07	6.20	454	552	2.9	5.1	32	2	34
C19-1	HR-13	9.5	+132	0.12	6.36	554	682	10.5	14.7	7	0	7
C9-1	HR-14	8.0	+192	0.11	6.30	522	607	13.4	14.6	24	0	24
C12-1	HR-15	9.0	+195	0.08	6.40	404	589	20.4	24.2	5	0	5
L8-1	HR-16	9.0	+215	0.08	6.60	411	571	15.6	17.9	54	0	54

[a]Tested at 289°C at a strain rate of 1.65 x 10^{-7} s^{-1} in simulated BWR water containing ≈8 ppm DO.

Table 10. Compositional characteristics (composition in wt.%) of model austenitic stainless steels irradiated to fluence of ≈0.3 x 10^{21} n·cm^{-2} (E > 1 MeV) correlated with results of SSRT[a] test and SEM fractography (HP = high purity, CP = commercial purity).

Alloy ID	Ni	Si	P	S	Mn	C	N	Cr	Mo/Nb	Remark	YS (MPa)	UTS (MPa)	UE (%)	TE (%)	TGSCC (%)	IGSCC (%)	TG+IGSCC (%)
C1	8.12	0.50	0.038	0.002	1.00	0.060	0.060	18.11	-	Low S, CP 304	490	680	13.4	16.6	4	0	4
L5	9.66	0.90	0.113	0.028	0.47	0.006	0.033	21.00	-	High P, Cr; Low C	513	539	29.5	32.7	2	2	4
L22	13.30	0.24	0.015	0.004	0.40	0.003	0.001	16.10	Mo 2.04	HP 316L, low Si, N	360	596	6.6	9.4	50	15	65
C3	8.91	0.46	0.019	0.004	1.81	0.016	0.083	18.55	-	CP 304L, Low Si	338	491	27.7	31.6	5	0	5
C16	12.90	0.38	0.014	0.002	1.66	0.020	0.011	16.92	-	High Ni; Low Si, S	370	527	17.6	20.6	2	0	2
L4	10.20	0.94	0.031	0.010	1.75	0.110	0.002	15.80	-	High Ni, Mn, C; Low N	367	542	19.7	22.3	38	0	38
L18	8.13	0.14	0.016	0.033	1.13	0.080	0.001	18.00	-	Low Si, N	503	572	6.3	8.8	54	0	54
C10	8.13	0.55	0.033	0.002	1.00	0.060	0.086	18.19	-	Low S, CP 304	523	640	17.4	18.9	6	0	6
C21	10.24	0.51	0.034	0.001	1.19	0.060	0.020	16.28	Mo 2.08	CP 316	480	620	15.9	19.4	4	0	4
L11	8.15	0.47	0.097	0.009	1.02	0.014	0.004	17.40	-	High P; Low Si, C, S, N	487	599	2.3	3.8	62	0	62
L13	8.18	1.18	0.027	0.022	0.36	0.026	0.001	17.40	-	High Si; Low Mn, C, N	248	461	22.1	24.8	8	0	8
L20	8.91	0.17	0.010	0.004	0.41	0.002	0.002	18.10	-	HP 304L, Low Si, N	454	552	2.9	5.1	32	2	34
C19	8.08	0.45	0.031	0.003	0.99	0.060	0.070	18.21	-	Low Si, S	554	682	10.5	14.7	7	0	7
C9	8.75	0.39	0.013	0.013	1.72	0.062	0.065	18.48	-	Low Si; High Mn	522	607	13.4	14.6	24	0	24
C12	8.23	0.47	0.018	0.002	1.00	0.060	0.070	18.43	-	Low Si, P, S	404	589	20.4	24.2	5	0	5
L8	10.20	0.15	0.093	0.010	1.85	0.041	0.001	18.30	-	High Ni, P, Mn; Low Si, N	411	571	15.6	17.8	64	0	64

[a]Test at 289°C at a strain rate of 1.65 x 10^{-7} s^{-1} in simulated BWR water; DO ≈8 ppm.

Table 11. Results of SSRT[a] test and SEM fractography for model austenitic stainless steels irradiated in helium at 289°C to a fluence of ≈0.9 x 10^{21} n·cm^{-2} (E > 1 MeV)

Specimen Ident. No.	SSRT No.	Feedwater Chemistry: Oxygen Conc. (ppm)	Feedwater Chemistry: Average ECP (mV SHE)	Feedwater Chemistry: Cond. at 25°C (μS·cm^{-1})	Feedwater Chemistry: pH at 25°C	SSRT Parameter: Yield Stress (MPa)	SSRT Parameter: Max. Stress (MPa)	SSRT Parameter: Uniform Elong. (%)	SSRT Parameter: Total Elong. (%)	Fracture Behavior: TGSCC (%)	Fracture Behavior: IGSCC (%)	Fracture Behavior: TGSCC + IGSCC (%)
L22-02	HR-17	8.0	+181	0.08	6.77	475	549	4.20	5.82	30	35	65
L11-02	HR-18	8.0	+191	0.08	6.55	820	856	0.43	1.65	50	14	64
L18-02	HR-19	8.0	+193	0.10	6.07	710	755	3.98	5.05	38	14	52
L20-02	HR-28		test in	289°C air		826	845	0.31	2.09	0	0	0
L20-05	HR-26	9.0	+182	0.09	6.32	670	743	0.37	1.03	0	0	0
L20-06	HR-27	8.0	+274	0.07	6.05	632	697	0.85	2.72	0	0	0
C9-02	HR-21	8.0	+240	0.07	6.47	651	679	1.42	2.50	62	22	84
L17-02	HR-22	8.0	+198	0.07	6.42	574	654	2.02	3.08	44	41	85
L7-02	HR-23	8.0	+215	0.07	6.03	553	561	0.24	2.44	38	54	92
C10-02	HR-24	7.0	+221	0.07	5.26	651	706	6.35	9.25	14	0	14
C3-02	HR-25	8.0	+240	0.07	6.34	632	668	16.72	19.74	9	4	13
C19-02	HR-30		test in	289°C air		888	894	6.41	10.21	1	0	1
C19-04	HR-31	8.0	+252	0.07	6.18	750	769	6.06	8.79	1	0	1
L6-02	HR-32	8.0	+250	0.07	6.40	493	546	2.45	3.77	8	27	35
L14-02	HR-33	8.0	+246	0.08	6.07	649	684	1.90	4.67	84	2	86
L13-02	HR-34	7.0	+222	0.09	6.85	602	624	1.67	4.95	55	2	57
L04-02	HR-35	7.0	+259	0.08	6.54	634	680	1.07	2.02	68	2	70
L05-02	HR-36	7.0	+243	0.07	6.85	665	725	3.07	4.57	3	5	8
C16-02	HR-37	7.0	+230	0.07	6.62	562	618	11.99	15.80	7	1	8
L8-02	HR-38	8.0	+242	0.07	6.57	838	838	0.12	3.12	15	22	37
C21-02	HR-39	8.0	+231	0.08	6.21	643	716	15.38	18.30	1	2	3
L2-02	HR-40	7.0	+239	0.07	7.11	839	849	0.88	1.56	38	4	42
L24-02	HR-41	8.0	+239	0.06	6.40	725	725	0.15	2.45	2	1	3
L23-02	HR-42	7.0	+237	0.08	6.60	787	818	0.38	1.24	3	24	27
C12-02	HR-43	7.0	+227	0.07	6.19	747	756	14.96	18.57	4	0	4
C1-02	HR-44	8.0	+229	0.07	6.30	707	763	13.36	17.04	2	0	2

[a]Tested at 289°C at a strain rate of 1.65 x 10^{-7} s^{-1} in simulated BWR water containing ≈8 ppm DO.

Table 12. Compositional characteristics (composition in wt.%) of model austenitic stainless steels irradiated to fluence of ≈0.9 x 10^{21} n·cm^{-2} (E > 1 MeV) correlated with results of SSRT[a] test and SEM fractography

Specimen ID	Ni	Si	P	S	Mn	C	N	Cr	O, B, Mo, Nb	Remarks[b]	YS (MPa)	UTS (MPa)	UE (%)	TE (%)	TGSCC (%)	IGSCC (%)	TG+IGSCC (%)
L22-02	13.30	0.024	0.015	0.004	0.40	0.003	0.001	16.10	Mo 2.04	HP 316L; low Si, N, S	475	549	4.20	5.82	30	35	65
L11-02	8.15	0.47	0.097	0.009	1.02	0.014	0.004	17.40	-	high P; low Si, C, S, N	820	856	0.43	1.65	50	14	64
L18-02	8.13	0.14	0.016	0.033	1.13	0.080	0.001	18.00	-	low Si, N	710	755	3.98	5.05	38	14	52
L20-05	8.91	0.017	0.010	0.004	0.41	0.002	0.002	18.10	O 0.0940	high O; low Si, N; HP 304L	670	743	0.37	1.03	dendritic structure		
L20-06	8.91	0.017	0.010	0.004	0.41	0.002	0.002	18.10	O 0.0940	highO; low Si, N; HP 304L	632	697	0.85	2.72	dendritic structure		
C9-02	8.75	0.39	0.013	0.013	1.72	0.062	0.065	18.48	-	low Si; high Mn	651	679	1.42	2.50	62	22	84
L17-02	8.00	0.66	0.090	0.009	0.48	0.061	0.078	15.30	O 0.0090	high P; low Cr, Mn, S	574	654	2.02	3.08	44	41	85
L7-02	10.60	0.18	0.040	0.038	1.02	0.007	0.111	15.40	O 0.0274	high S, N, O; low Si, C	553	561	0.24	2.44	38	54	92
C10-02	8.13	0.55	0.033	0.002	1.00	0.060	0.086	18.19	-	CP 304; low S; high N	651	706	6.35	9.25	14	0	14
C3-02	8.91	0.46	0.019	0.004	1.81	0.016	0.083	18.55	-	CP 304L; high Mn, N; low S	632	668	16.72	19.74	9	4	13
C19-04	8.08	0.45	0.031	0.003	0.99	0.060	0.070	18.21	O 0.0200	CP 304; low S	750	769	6.06	8.79	1	0	1
L6-02	10.00	1.90	0.020	0.005	1.13	0.096	0.087	17.10	O 0.0058	high Si; low S	493	546	2.45	3.77	8	27	35
L14-02	7.93	1.49	0.080	0.002	1.76	0.107	0.028	15.00	O 0.0045	high Si, P, Mn; low Cr, S	649	684	1.90	4.67	84	2	86
L13-02	8.18	1.18	0.027	0.022	0.36	0.026	0.001	17.40	-	high Si, S; Low Mn, C, N	602	624	1.67	4.95	55	2	57
L4-02	10.20	0.94	0.031	0.010	1.75	0.110	0.002	15.80	-	high Si, C; low N, Cr	634	680	1.07	2.02	68	2	70
L5-02	9.66	0.90	0.113	0.028	0.47	0.006	0.033	21.00	-	high Si, P, Cr; Low Mn, C	665	725	3.07	4.57	3	5	8
C16-02	12.90	0.38	0.014	0.002	1.66	0.020	0.011	16.92	0.0157	high Ni; low P, S, C	562	618	11.99	15.80	7	1	8
L8-02	10.20	0.15	0.093	0.010	1.85	0.041	0.001	18.30	-	high P, Mn; low Si, N	838	838	0.12	3.12	15	22	37
C21-02	10.24	0.51	0.034	0.001	1.19	0.060	0.020	16.28	Mo 2.08	CP 316, low S	643	716	15.38	18.30	1	2	3
L2-02	10.50	0.82	0.080	0.034	1.58	0.074	0.102	17.02	O 0.0066	high O, P, S, N	839	849	0.88	1.56	38	4	42
L24-02	12.30	0.03	0.007	0.005	0.48	0.031	0.002	16.90	Nb 1.72 O 0.0129	HP 348L; low Si, P, S, C, N	725	725	0.15	2.45	2	1	3
L23-02	12.04	0.68	0.030	0.047	0.96	0.043	0.092	17.30	Nb 1.06 O 0.0093	CP 348, high S	787	818	0.38	1.24	3	24	27
C12-02	8.23	0.47	0.018	0.002	1.00	0.060	0.070	18.43	-	304, low S, low P	747	756	14.96	18.57	4	0	4
C1-02	8.12	0.50	0.038	0.002	1.00	0.060	0.060	18.11	-	304, low S	707	763	13.36	17.04	2	0	2

[a]Test at 289°C at a strain rate of 1.65 x 10^{-7} s^{-1} in simulated BWR water; DO ≈8 ppm.
[b]HP = high purity, CP = commercial purity.

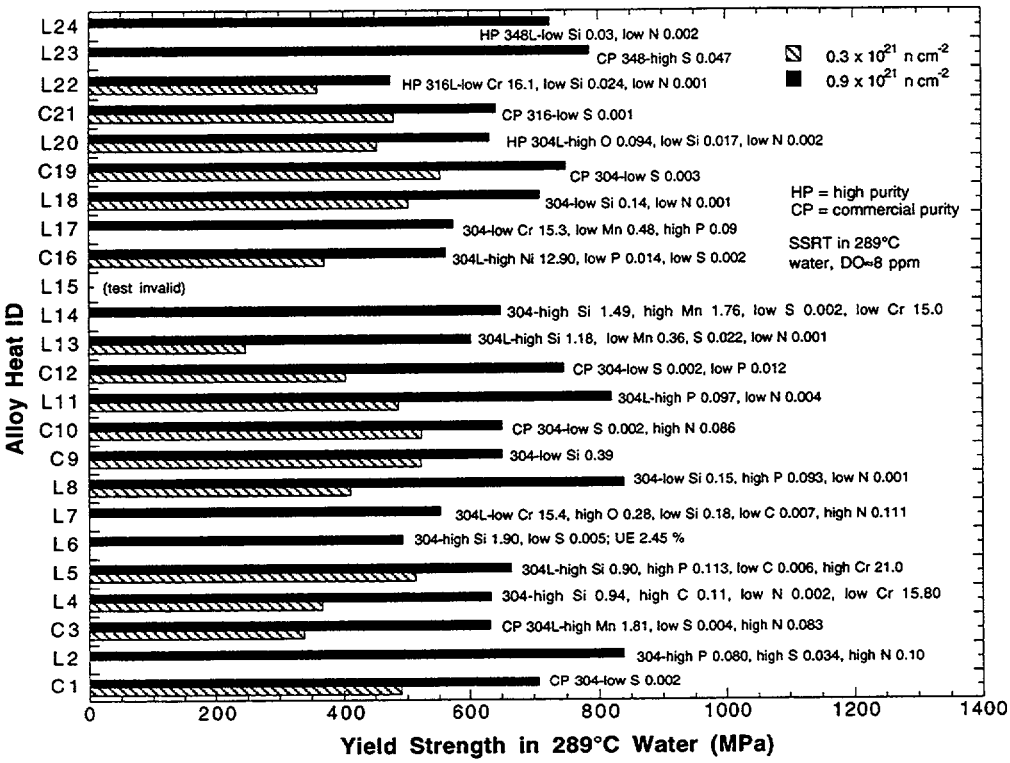

Fig. 2. Effects of fluence on yield strength measured in 289°C water containing ≈8 ppm DO.

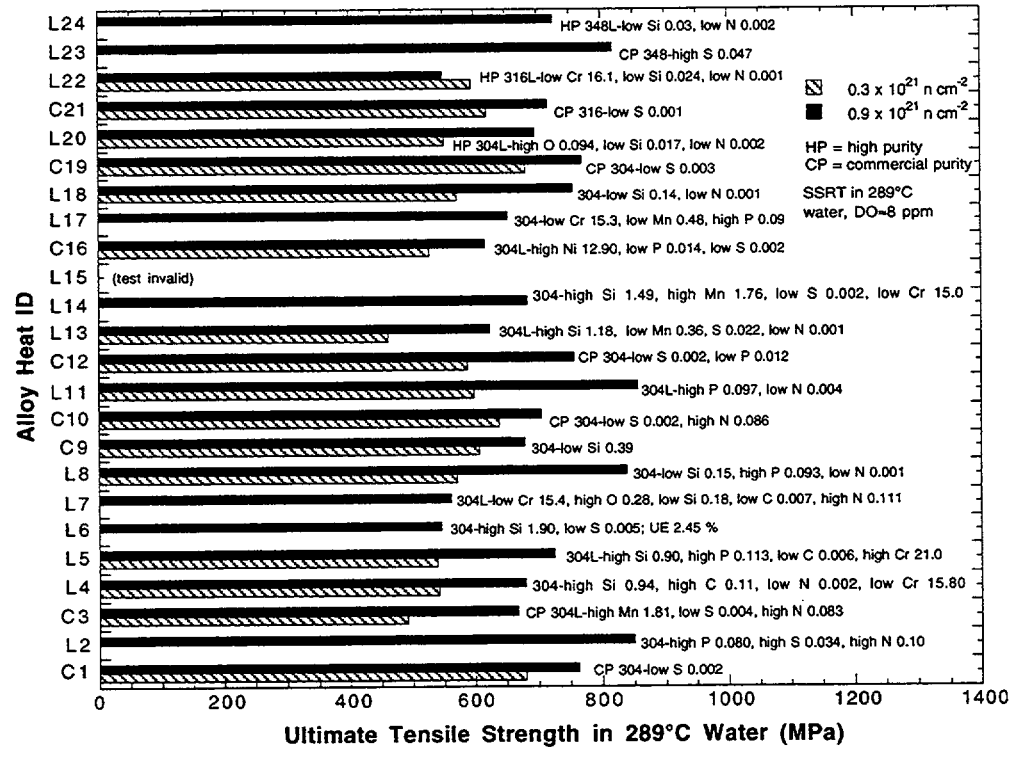

Fig. 3. Effects of fluence on maximum strength measured in 289°C water containing ≈8 ppm DO.

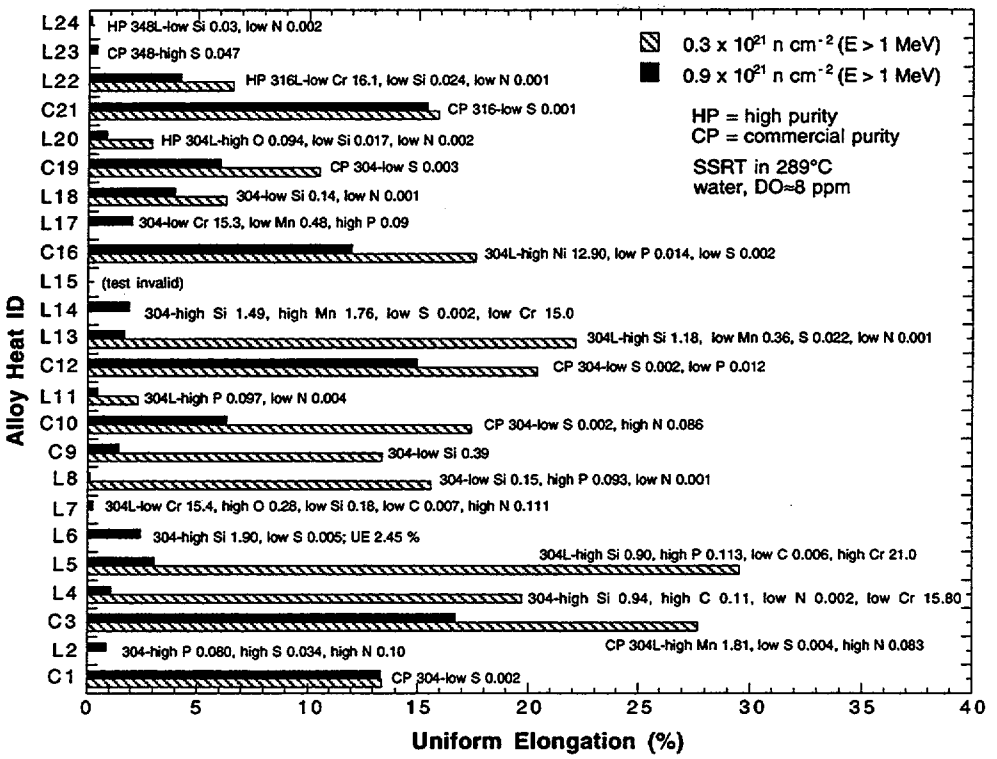

Fig. 4. Effects of fluence on uniform elongation measured in 289°C water containing ≈8 ppm DO.

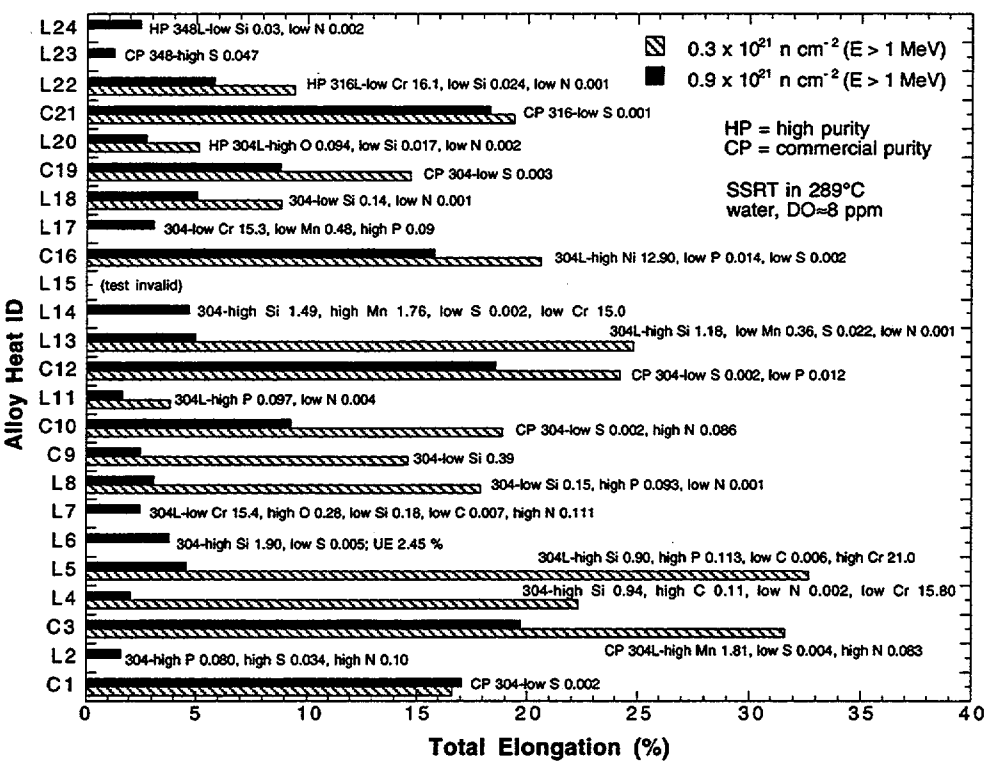

Fig. 5. Effects of fluence on total elongation measured in 289°C water containing ≈8 ppm DO.

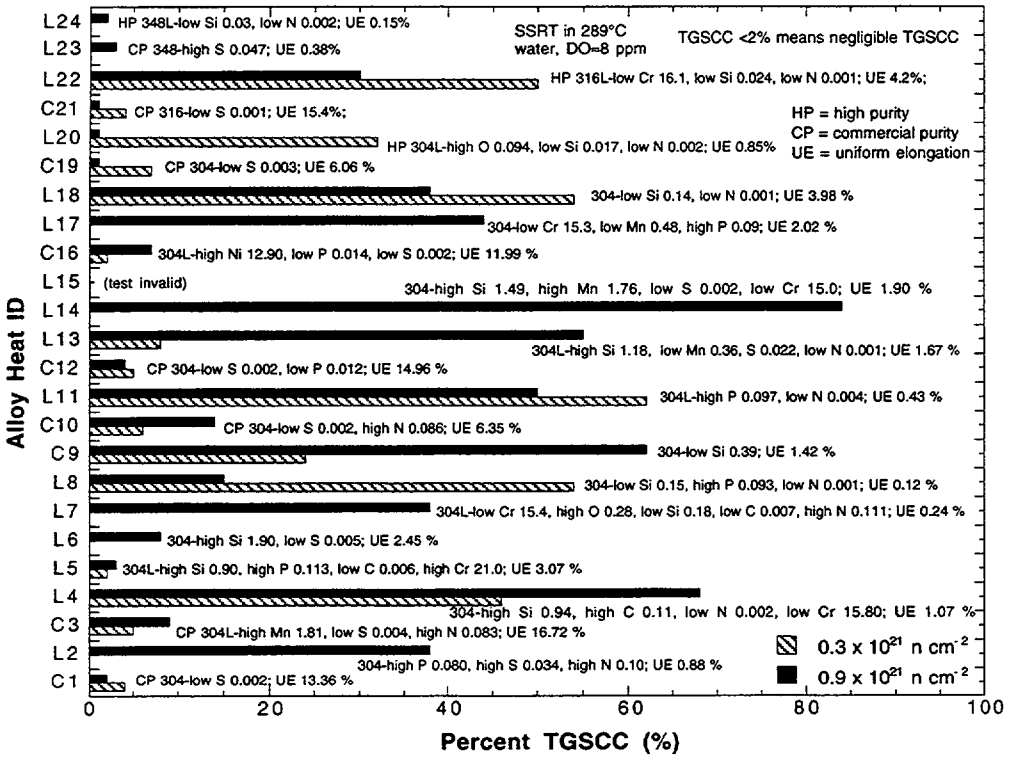

Fig. 6. Effects of fluence on percent TGSCC measured in 289°C water containing ≈8 ppm DO.

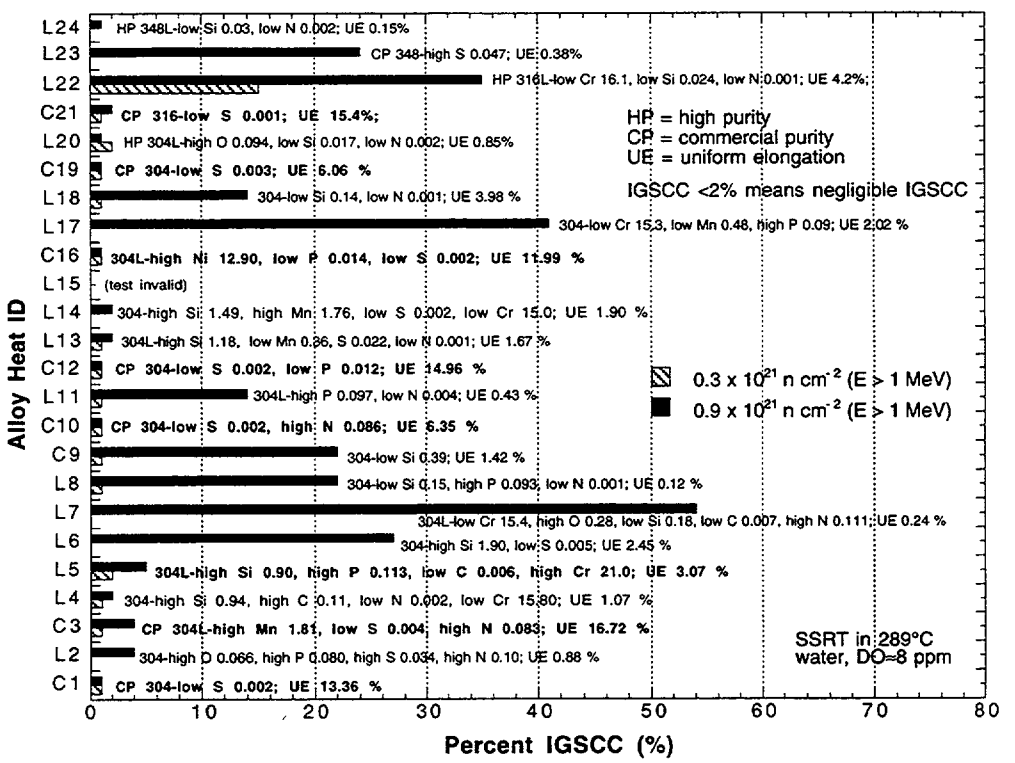

Fig. 7. Effects of fluence on percent IGSCC measured in 289°C water containing ≈8 ppm DO.

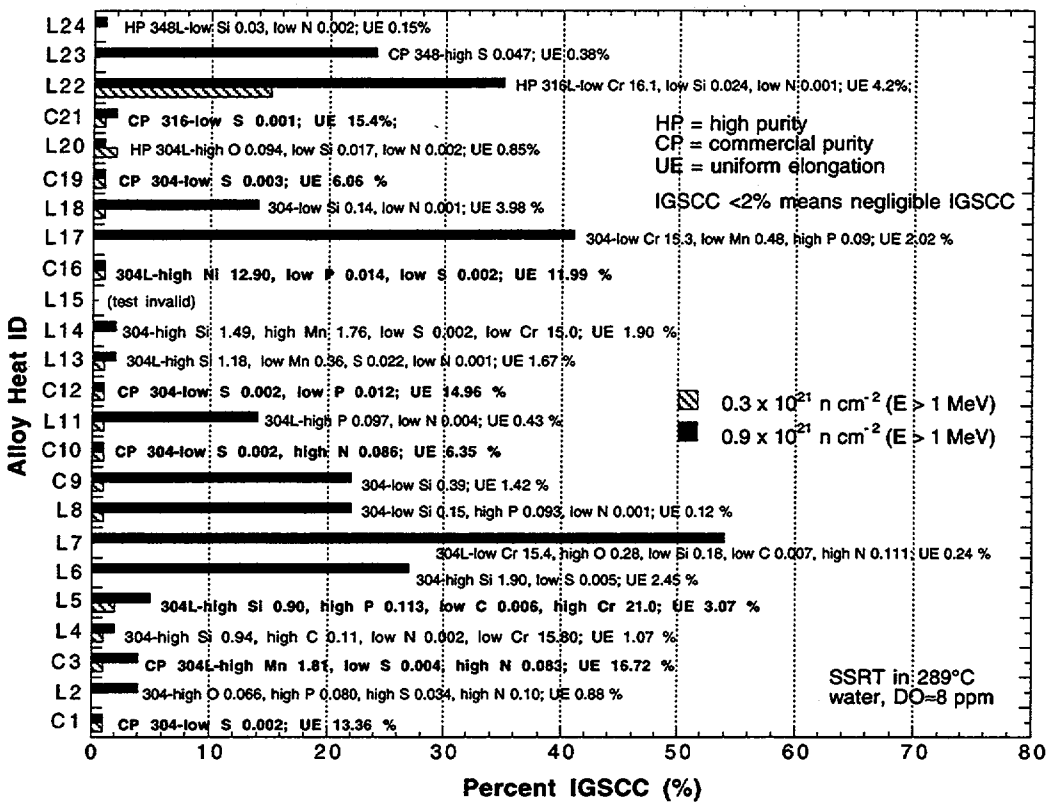

Fig. 8. Effects of fluence on percent TGSCC + IGSCC measured in 289°C water containing ≈8 ppm DO.

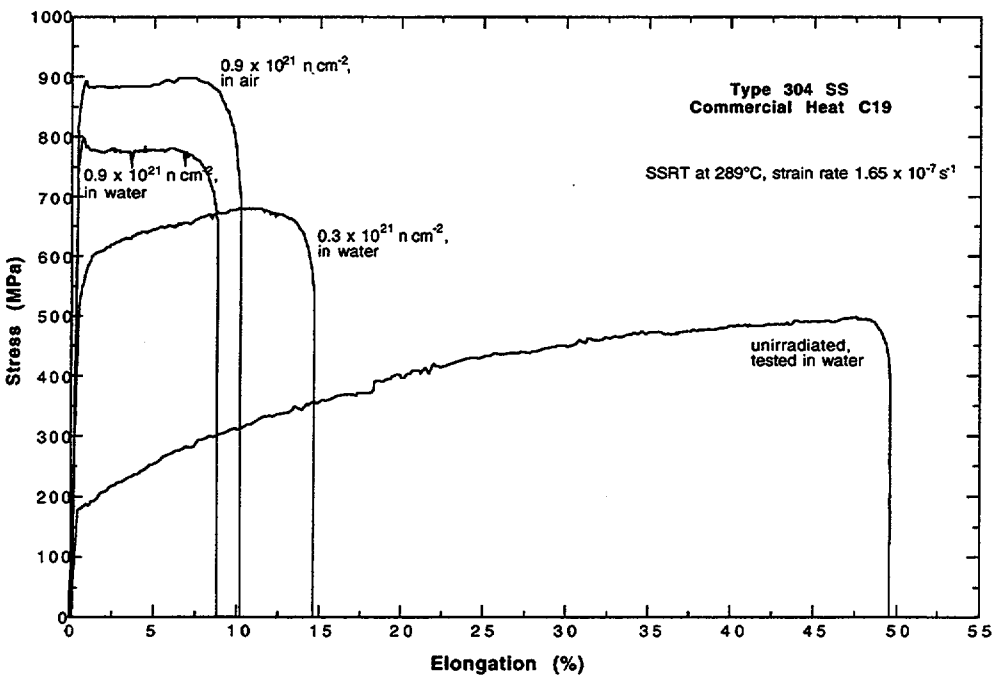

Fig. 9. Effects of fluence and test environment on load elongation behavior of Type 304 SS commercial heat C19.

Results of the SEM fractography (see Figs. 6-8) show that when fluence increased from $\approx 0.3 \times 10^{21}$ n·cm^{-2} to $\approx 0.9 \times 10^{21}$ n·cm^{-2}, the percent TGSCC in some alloys decreased, and at the same time, the percent IGSCC increased, e.g., Alloys L22, L18, L11, and L8. The IGSCC fracture surfaces in these alloys were surrounded by TGSCC fracture surfaces This indicates that an IGSCC fracture surface emerges from a portion of a TGSCC fracture surface and that for many alloys, high susceptibility to TGSCC is a precursor to susceptibility to IGSCC at a higher fluence. However, the threshold fluence for the transition from TGSCC to IGSCC appears to differ significantly from alloy to alloy.

4.2 Effect of Sulfur

Based on the information given in Tables 8, 10, and 12, we examined the relationship between the fracture properties and the compositional characteristics of the alloys to identify the alloying and impurity elements that significantly influence stress corrosion cracking behavior. In the unirradiated state or after irradiation to $\approx 0.3 \times 10^{21}$ n·cm^{-2}, commercial and laboratory heats of Types 304, 304L, and 348 SS that contain relatively high concentrations of S (>0.009 wt.% S, 15-18.50 wt.% Cr) exhibited significant susceptibility to TGSCC, whereas alloys that contain a relatively low concentration of S (<0.005 wt.% S) exhibited good resistance to TGSCC. These relationships are shown in Fig. 10.

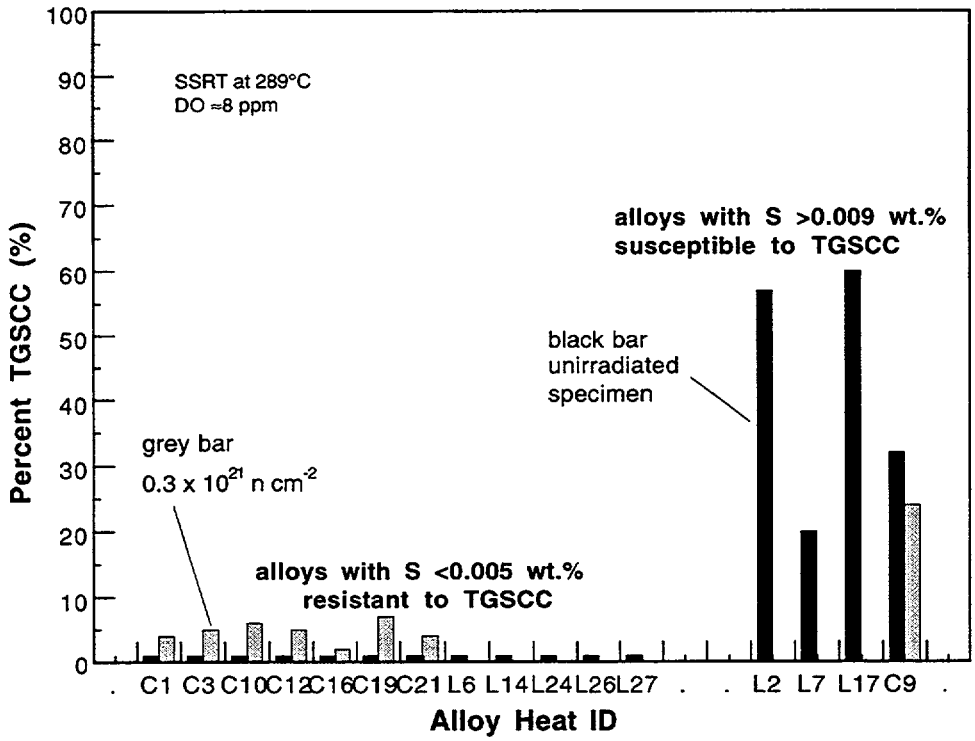

Fig. 10. Effect of S on susceptibility to TGSCC of two groups of alloys in unirradiated state or after irradiation to ≈0.3 x 10^{21} n·cm^{-2} (E > 1 Mev); one group contains low concentrations of S (<0.005 wt.%) and the other contains relatively high concentrations of S (>0.009 wt.%).

At ≈0.9 x 10^{21} n·cm^{-2}, commercial heats of Types 304 and 316 SS that contain low concentrations of S (<0.004 wt.% S) exhibited high resistance to TGSCC and IGSCC (see Fig. 11) and high uniform and total elongation (see Fig. 12), whereas a commercial heat of Type 304 SS that contains a relatively high concentration of S (≈0.013 wt.% S) exhibited poor resistance to TGSCC and IGSCC (Fig. 11) and low uniform and total elongation (Fig. 12). Susceptibilities of the high-S heat C19 to TGSCC were high in unirradiated state and after irradiation to low fluence (see Fig. 10).

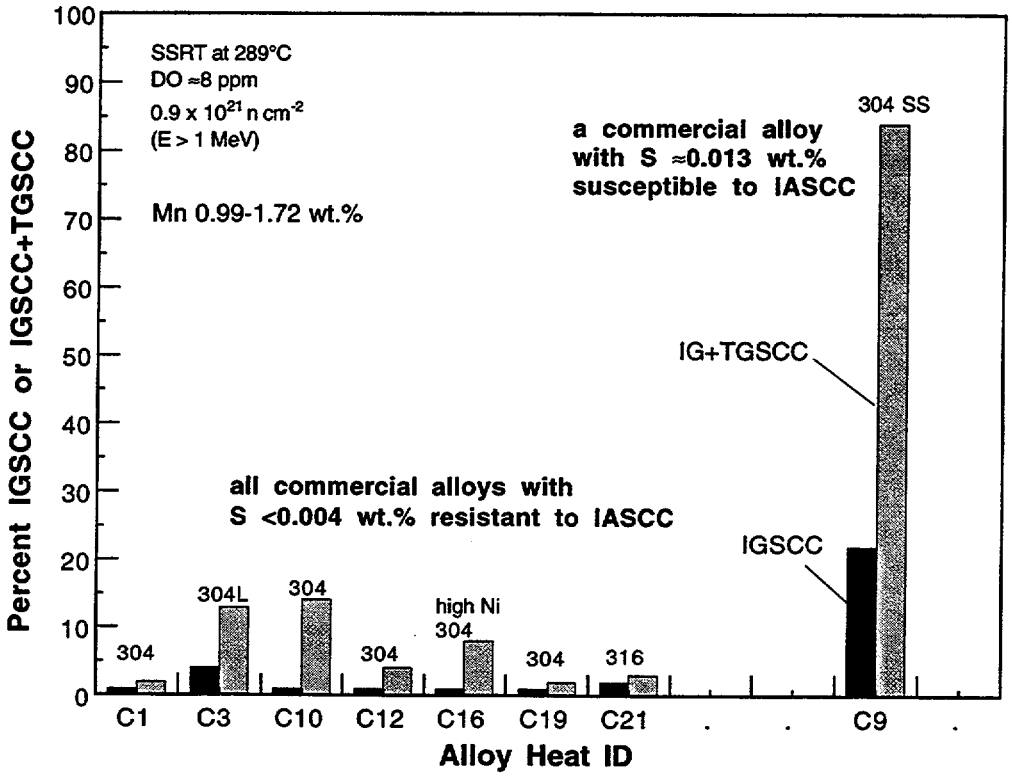

Fig. 11. Effect of S on susceptibility to TGSCC and IGSCC of commercial alloys measured after irradiation to ≈0.9 x 10^{21} n·cm^{-2} (E > 1 MeV); one Group of alloys contain low concentrations of S (<0.004 wt.%) and the other alloy contains relatively high concentrations of S (>0.013 wt.%).

The observations summarized in Figs. 10-12 indicate strongly that for commercial heats of Types 304 and 304L SS, a high concentration of S (>0.009 wt.%) is significantly detrimental and that a sufficiently low concentration of S (e.g., <0.004 wt.%) is a necessary condition for good resistance to IASCC.

From an earlier study on steels irradiated to ≈2.5 x 10^{21} n·cm^{-2} (E > 1 MeV) in a BWR, Kasahara et al.[16] reported that the effect of high concentrations of S on IASCC susceptibility was significant for one heat of Type 316L SS that contained 0.035 wt.% S, whereas for a similar heat of Type 316L SS that contained 0.001 wt.% S, susceptibility to IASCC was insignificant. However, a similar effect of the concentration of S was not observed for two heats of Type 304L SS. In other studies on steels irradiated to ≈0.67 x 10^{21} n·cm^{-2} (E > 1 MeV), Tsukada and Miwa reported deleterious effects of high concentrations of S for a heat of

Type 304L SS (0.032 wt.% S)[12] and a Ti-doped heat of Type 316 SS (0.037 wt.% S).[20] Although these earlier investigations were conducted only on a limited number of heats, the results appear to be consistent with the present observation that an S concentration as low as ≈0.009 wt.% could be deleterious to the susceptibility of steel to TGSCC and IGSCC.

The exact mechanism of how a high concentration of S in Types 304, 304L, or 316 SS leads to higher susceptibilities to TGSCC and IGSCC, as observed in this study, is not clear. In a previous investigation, grain-boundary concentrations of S in BWR neutron absorber tubes and control blade sheath fabricated from several high- and commercial-purity heats of Types 304 and 304L SS and irradiated to ≈2.6 x 10^{21} n·cm^{-2} (E > 1 MeV) were determined by Auger electron spectroscopy (AES).[14] However, because of S contamination that occurs during the process of anodic charging of H into the specimen prior to analysis by AES (which is necessary to induce intergranular fracture in vacuum in an Auger electron microscope and hence reveal grain boundaries of the specimen), a good correlation could not be established between grain-boundary S concentration and susceptibility to IGSCC of the BWR neutron absorber tubes and control blade sheath.

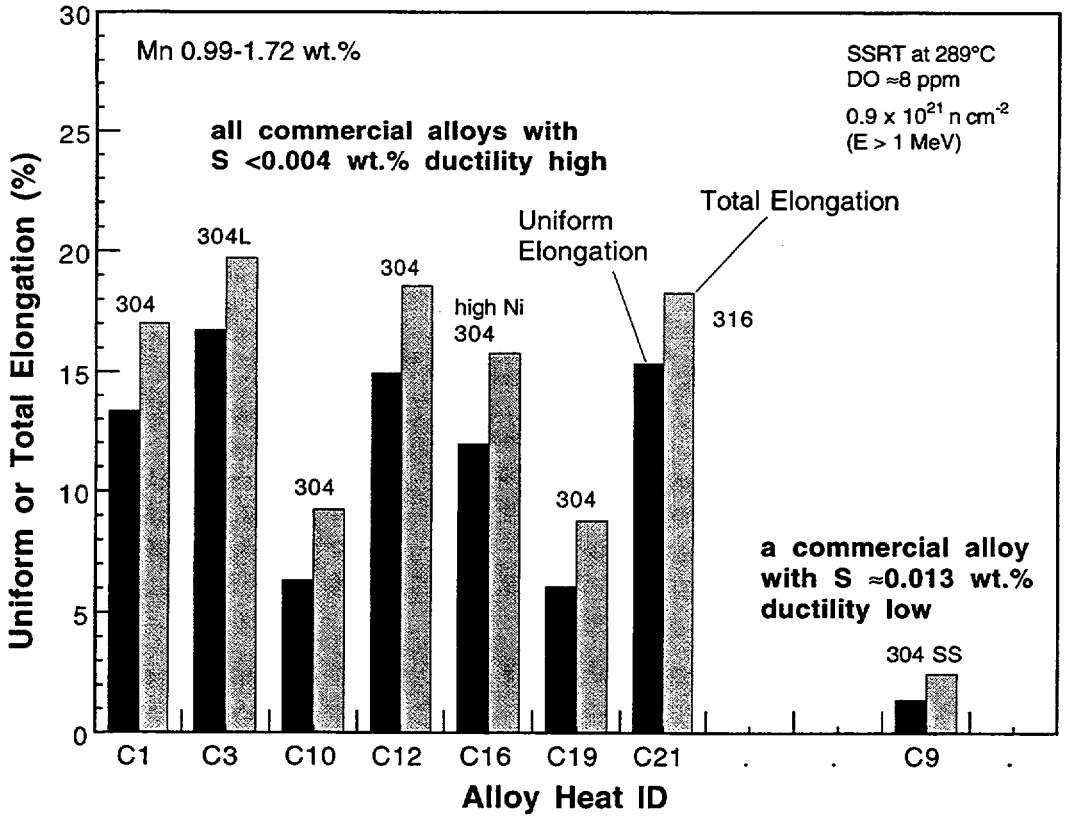

Fig. 12. Effect of S on uniform and total elongation of commercial alloys measured after irradiation to ≈0.9 x 10^{21} n·cm^{-2} (E > 1 MeV); one group of alloys contain low concentrations of S (<0.004 wt.%); the other alloy contains a relatively high concentration of S (>0.013 wt.%).

Grain-boundary segregation of S in irradiated steels is also difficult to determine by energy-dispersive spectroscopy (EDS) in a transmission electron or analytical electron microscope (TEM or AEM). Furthermore, several factors complicate the exact distribution of S in irradiated steels, i.e., trapping of S in MnS and other sulfide precipitates, potential dissolution of MnS and other sulfides in BWR-like water,[21] and irradiation-induced modification of the composition and morphology of MnS precipitates.[22] Therefore, it is not surprising that a good correlation could not be established between grain-boundary S concentration and susceptibility of irradiated steels to IGSCC.

For unirradiated steels, thermally induced grain-boundary segregation of S has been measured by AES by Andresen and Briant[23] for one heat of Type 304L and one heat of 316NG SS that contained 0.030-0.037 wt.% S and were annealed at 400-700°C. Susceptibility of both materials to IGSCC was significant. The former material did not contain any Mn; therefore, IGSCC in that material was attributed to grain-boundary segregation of S. The lower percent IGSCC observed for the latter material, which contained 1.1 wt.% Mn and 0.067 wt.% P, was attributed to lower grain-boundary segregation of S that may have occurred in the material because P and S must compete for grain-boundary sites for segregation.

A similar model, based on irradiation-induced grain-boundary segregation of S, does not appear to be consistent with the present observation that a higher concentration of S is conducive to higher susceptibilities to TGSCC and IGSCC. Conclusive evidence for irradiation-induced grain-boundary segregation of S does not appear to have been established. As pointed out previously, the IGSCC fracture surface in high-S steels was often observed in the middle of and surrounded by TGSCC fracture surface. This finding appears to indicate that MnS, and possibly other soluble sulfides that may have more complex chemical compositions, dissolves in crack tip water that initially advances via TGSCC and then releases into the crack-tip crevice water deleterious ions that are conducive to producing IGSCC. To identify the exact processes and mechanisms, SSRT tests on higher fluence specimens and a systematic microstructural investigation will be helpful.

4.3 Effect of Chromium

At a fluence of $\approx 0.9 \times 10^{21}$ n·cm^{-2}, a laboratory alloy that contains an unusually high concentration of Cr (≈21 wt.%) exhibited excellent resistance to TGSCC and IGSCC, in spite of high S content (≈0.028 wt.% S). In contrast to this, several heats containing relatively low concentrations of Cr of <17.5 wt.% exhibited significant susceptibility to TGSCC and IGSCC (see Fig. 13). This observation indicates that Cr atoms in high concentration play a major role in suppressing susceptibility to IASCC under BWR conditions.

4.4 Effect of Silicon

Yield strength of the model alloys, measured in BWR-like water at 289°C, was nearly constant at ≈200 MPa in unirradiated state and was more or less independent of Si concentration (see Fig. 14). However, as fluence was increased to $\approx 0.3 \times 10^{21}$ n·cm^{-2} and $\approx 0.9 \times 10^{21}$ n·cm^{-2}, the degree of increase in yield strength was significantly lower for alloys that contain >0.9 wt.% Si than for alloys that contain <0.8 wt.% Si (Fig. 14). This finding indicates

that nature of irradiation-induced hardening centers and the degree of irradiation hardening are significantly influenced by alloy Si content. Silicon atoms in austenitic stainless steels occupy substitutional sites; therefore, they are likely to interact preferentially with irradiation-induced vacancy sites in the steel. This effect is likely to inhibit the formation of vacancy clusters or vacancy-impurity complexes, and is, therefore, conducive to a less significant irradiation-induced hardening. An effect similar to that of Si was, however, not observed for C and N.

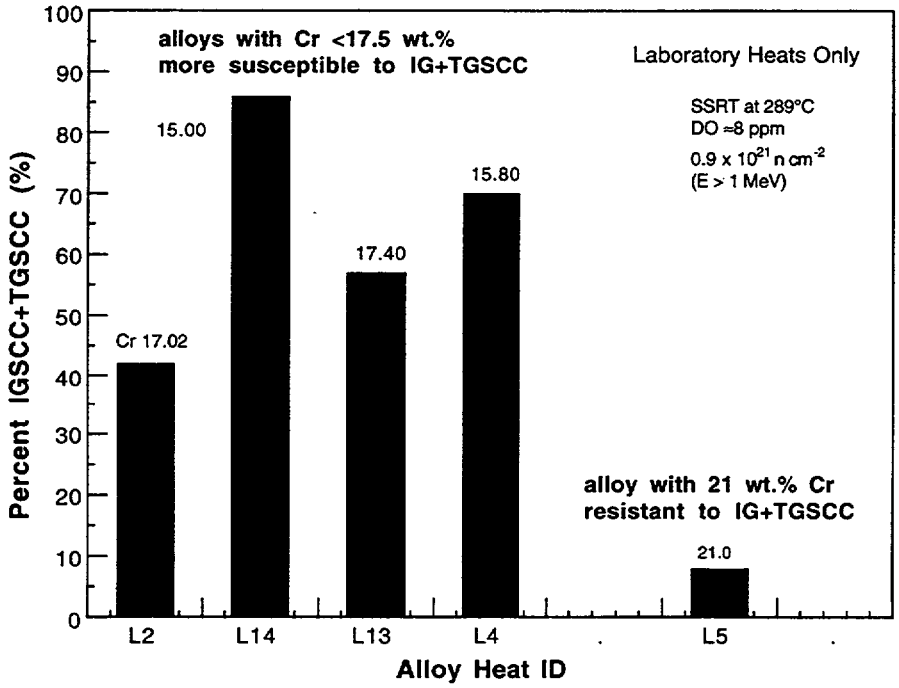

Fig. 13. Effect of Cr on susceptibility to TGSCC and IGSCC of laboratory alloys measured after irradiation to ≈0.9 x 10^{21} n·cm^{-2} (E > 1 MeV); alloys susceptible to IASCC contain relatively low concentrations of Cr (<17.4 wt.%); an alloy resistant to IASCC contains relatively high concentrations of Cr (≈21.0 wt.%).

Among laboratory heats of Types 304 and 304L SS, alloys that contain <0.67 wt.% Si exhibited significant susceptibility to IGSCC, whereas alloys with 0.8-1.5 wt.% Si exhibited negligible susceptibility to IGSCC. However, an alloy with ≈1.9 wt.% Si exhibited some degree of susceptibility to IGSCC (percent IGSCC ≈ 27). These observations indicate that an Si concentration of ≈0.8 to ≈1.5 wt.% is beneficial in delaying the onset of or suppressing the susceptibility to IASCC. To determine if similar effects are evident at higher fluence levels would require testing of the high-fluence specimens that will be discharged after irradiation to ≈2.0 x 10^{21} n·cm^{-2} (E > 1 MeV).

Consistent with the beneficial effects of Cr and Si and the deleterious effect of S discussed above, an alloy (L7) that contains an unusually low concentrations of Cr (15.4 wt.%) and Si (0.18 wt.%) and an unusually high concentration of S (0.038 wt.%) exhibited the worst susceptibility to IASCC at ≈0.9 x 10^{21} n·cm^{-2} (i.e., ≈54% IGSCC, ≈92% TGSCC+IGSCC). Alloy L7 also contained an unusually high concentration of O (0.027 wt.%). Considering deleterious

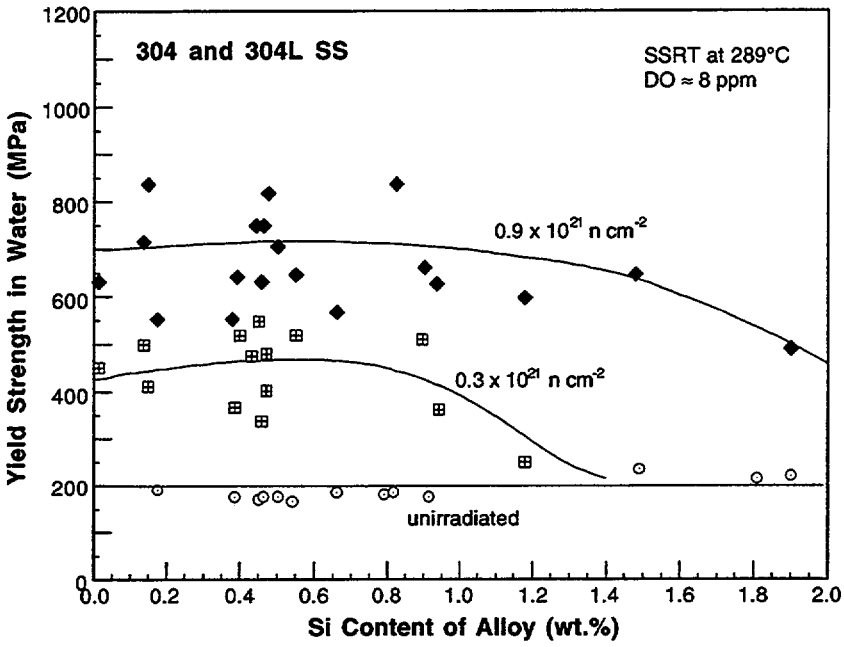

Fig. 14. Effect of Si concentration on yield strength of Types 304 and 304L alloys measured in 289°C water before and after irradiation.

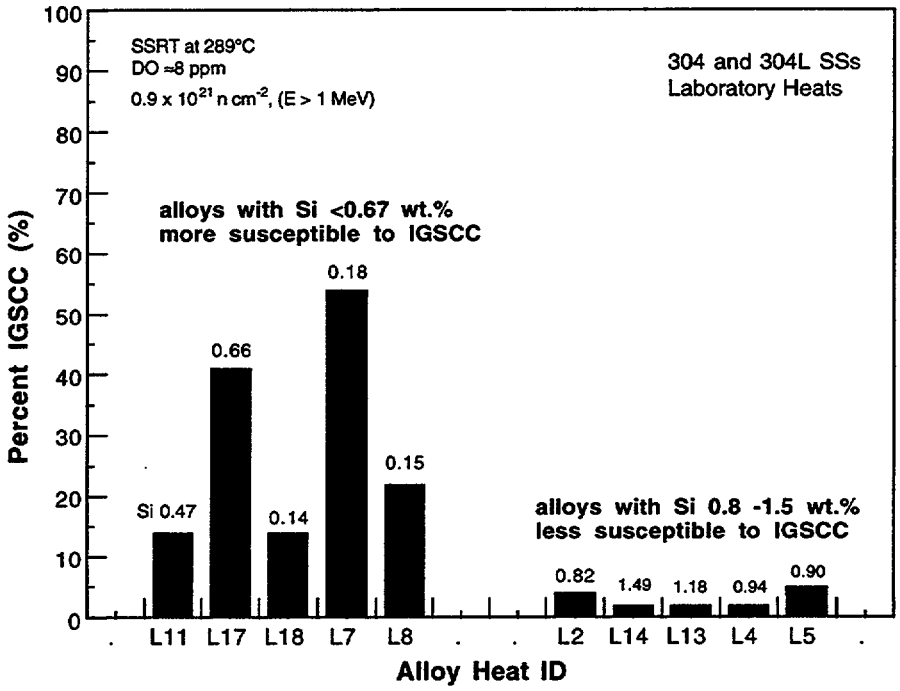

Fig. 15. Effect of Si on susceptibility to IGSCC of laboratory alloys of Types 304 and 304L SS measured after irradiation to ≈0.9 x 10^{21} n·cm^{-2} (E > 1 MeV); alloys susceptible to IASCC contain relatively low concentrations of Si (<0.67 wt.%); alloys resistant to IASCC contain relatively high concentrations of Si (0.8-1.5 wt.%).

effect of O,[14,15] the unusually high concentration of O is believed to be one of the important factors that led to the poor performance of the alloy. Alloy L7 exhibited significant susceptibility to TGSCC (≈20% TGSCC) in water even in unirradiated state (see Table 7). These observations suggest that to avoid high susceptibility to IASCC, it is important to ensure sufficiently low concentrations of S and O and a sufficiently high concentration of Si.

4.5 Work-Hardening Capability

Although susceptibilities to TGSCC and IGSCC were insignificant and the fracture surface morphology was mostly ductile, some laboratory-fabricated alloys exhibited very low uniform elongation and poor work-hardening capability in water after irradiation to $\approx 0.9 \times 10^{21}$ n·cm^{-2}, i.e., L20 (characterized by dendritic structure and very high O concentration), L8 (304 SS), L23 (348 SS), and L24 (348 SS). These alloys contained unusually high concentrations of O or unusually low concentrations of Si, or both. To better understand such behavior, which usually indicates severe susceptibility to dislocation channeling or other forms of localized deformation, a systematic microstructural investigation by transmission and scanning electron microscopies is desirable.

Laboratory alloys that contain unusually high concentrations of O exhibited either high susceptibility to IGSCC or poor work-hardening capability. Fracture surfaces of such alloys indicated that void coalescence and crack initiation are promoted at or near oxide inclusions that are in high density. Then, ductile tearing of remaining ridges occurs early, leading to low uniform and total elongations, indicating that careful control of O concentration, which is not specified in the ASTM Specifications for austenitic SSs, is a very important factor in minimizing susceptibility to IASCC.

5 Conclusions

(1) At ≈0.3 x 10^{21} n·cm^{-2}, many alloys were susceptible to transgranular stress corrosion cracking (TGSCC), but only one alloy of Type 316L SS that contains a very low concentration of Si (0.024 wt.%) was susceptible to intergranular stress corrosion cracking (IGSCC). Alloy-to-alloy variations in susceptibility to TGSCC were significant at ≈0.3 x 10^{21} n·cm^{-2}.

(2) As fluence was increased from ≈0.3 x 10^{21} n·cm^{-2} to ≈0.9 x 10^{21} n·cm^{-2}, IGSCC fracture surfaces emerged in many other alloys, usually in the middle of and surrounded by TGSCC fracture surfaces. This finding indicates that for many alloys, high susceptibility to TGSCC is a precursor to susceptibility to IGSCC at a higher fluence.

(3) Alloy-to-alloy variations in susceptibility to TGSCC and IGSCC were significant at ≈0.9 x 10^{21} n·cm^{-2}. Susceptibility to TGSCC and IGSCC was influenced by more than one alloying and impurity element in a complex manner.

(4) In unirradiated state and at the relatively low fluence level of ≈0.3 x 10^{21} n·cm^{-2}, commercial and laboratory heats of Types 304, 304L, and 348 SS that contain relatively high concentrations of S (>0.009 wt.% S, 15-18.50 wt.% Cr) exhibited significant susceptibility to TGSCC, whereas alloys that contain a relatively low concentration of S (<0.005 wt.%) exhibited good resistance to TGSCC At ≈0.9 x 10^{21} n·cm^{-2}, commercial heats of Types 304 and 316 SSs that contain low concentrations of S, exhibited high resistance to TGSCC and IGSCC and high levels of uniform and total elongation, whereas a commercial heat of Type 304 SS that contain a relatively high concentration of S exhibited poor resistance to TGSCC and IGSCC and low levels of uniform and total elongation. These observations indicate that for commercial heats of Types 304 and 304L SS, a high concentration of S (>0.009 wt.%) is significantly detrimental and that a sufficiently low concentration of S is a necessary condition to ensure good resistance to IASCC.

(5) At ≈0.9 x 10^{21} n·cm^{-2}, a laboratory alloy that contains a high concentration of Cr (≈21 wt.%) exhibited excellent resistance to TGSCC and IGSCC in spite of high S content (≈0.028 wt.% S), whereas heats with <17.5 wt.% Cr exhibited significant susceptibility to TGSCC plus IGSCC. This finding indicates that Cr atoms in high concentration play a major role in suppressing susceptibility to IASCC under BWR conditions.

(6) Yield strength of the model alloys, measured in BWR-like water at 289°C, was nearly constant at ≈200 MPa in the unirradiated state and was more or less independent of Si concentration. However, as the alloys were irradiated to ≈0.3 x 10^{21} n·cm^{-2} and ≈0.9 x 10^{21} n·cm^{-2}, the degree of increase in yield strength was significantly lower for alloys that contain >0.9 wt.% Si than for alloys that contain <0.8 wt.% Si. This observation indicates that the nature of irradiation-induced hardening centers and the degree of irradiation hardening are significantly influenced by alloy Si content. Similar influence of C and N was not observed.

(7) Among laboratory heats of Types 304 and 304L SS, alloys that contain <0.67 wt.% Si exhibited significant susceptibility to IGSCC, whereas heats with 0.8-1.5 wt.% Si exhibited

negligible susceptibility to IGSCC. However, an alloy with ≈1.9 wt.% Si exhibited some degree of susceptibility to IGSCC. These observations indicate that a Si content between ≈0.8 and ≈1.5 wt.% is beneficial in delaying the onset of or suppressing the susceptibility to IASCC. Consistent with the effects of S, Cr, and Si, an alloy that contains unusually low concentrations of Cr and Si and unusually high concentrations of S and O exhibited the worst susceptibility to IASCC at $\approx 0.9 \times 10^{21}$ n·cm^{-2}.

(8) Although susceptibility to TGSCC and IGSCC was insignificant and the fracture surface morphology was mostly ductile, some alloys exhibited very low uniform elongation and poor work-hardening capability in water after irradiation to $\approx 0.9 \times 10^{21}$ n·cm^{-2}. Such alloys contained unusually high concentrations of O or unusually low concentrations of Si or both. To better understand such behavior, usually indicative of severe susceptibility to dislocation channeling or other forms of localized deformation, a systematic microstructural investigation by transmission and scanning electron microscopy would be needed.

(9) A few alloys that contain unusually high concentrations of O exhibited either high susceptibility to IGSCC or poor work hardening capability. This finding indicates that careful control of O concentration is a very important factor in minimizing susceptibility to IASCC.

References

1. M. E. Indig, J. L. Nelson, and G. P. Wozadlo, "Investigation of Protection Potential against IASCC," in Proc. 5th Intl. Symp. on Environmental Degradation of Materials in Nuclear Power Systems – Water Reactors, D. Cubicciotti, E. P. Simonen, and R. Gold, eds., American Nuclear Society, La Grange Park, IL, 1992, pp. 941-947.

2. M. Kodama, S. Nishimura, J. Morisawa, S. Shima, S. Suzuki, and M. Yamamoto, "Effects of Fluence and Dissolved Oxygen on IASCC in Austenitic Stainless Steels," ibid., pp. 948-954.

3. H. M. Chung, W. E. Ruther, J. E. Sanecki, A. G. Hins, and T. F. Kassner, "Effects of Water Chemistry on Intergranular Cracking of Irradiated Austenitic Stainless Steels," in Proc. 7th Intl. Symp. on Environmental Degradation of Materials in Nuclear Power Systems - Water Reactors, G. Airey et al., eds., NACE International, Houston, 1995, pp. 1133-1143.

4. F. Garzarolli, P. Dewes, R. Hahn, and J. L. Nelson, "Deformability of High-Purity Stainless Steels and Ni-Base Alloys in the Core of a PWR," in Proc. 6th Intl. Symp. on Environmental Degradation of Materials in Nuclear Power Systems - Water Reactors, R. E. Gold and E. P. Simonen, eds., The Minerals, Metals, and Materials Society, Warrendale, PA, 1993, pp. 607-613.

5. H. Kanasaki, T. Okubo, I. Satoh, M. Koyama, T. R. Mager, and R. G. Lott, "Fatigue and Stress Corrosion Cracking Behavior of Irradiated Stainless Steels in PWR Primary Water," in Proc. 5th Intl. Conf. on Nuclear Engineering, March 26-30, 1997, Nice, France.

6. A. J. Jacobs, G. P. Wozadlo, K. Nakata, T. Yoshida, and I. Masaoka, "Radiation Effects on the Stress Corrosion and Other Selected Properties of Type-304 and Type-316 Stainless Steels," in Proc. 3rd Intl. Symp. Environmental Degradation of Materials in Nuclear Power Systems – Water Reactors, G. J. Theus and J. R. Weeks, eds., The Metallurgical Society, Warrendale, PA, 1988, pp. 673-680.

7. K. Fukuya, K. Nakata, and A. Horie, "An IASCC Study Using High Energy Ion Irradiation," in Proc. 5th Intl. Symp. on Environmental Degradation of Materials in Nuclear Power Systems – Water Reactors, D. Cubicciotti, E. P. Simonen, and R. Gold, eds., American Nuclear Society, La Grange Park, IL, 1992, 814–820.

8. H. M. Chung, W. E. Ruther, J. E. Sanecki, A. G. Hins, and T. F. Kassner, "Stress Corrosion Cracking Susceptibility of Irradiated Type 304 Stainless Steels," in Effects of Radiation on Materials: 16th Int. Symp., ASTM STP 1175, A. S. Kumar, D. S. Gelles, R. K. Nanstad, and T. A. Little, eds., American Society for Testing and Materials, Philadelphia, 1993, pp. 851-869.

9. H. M. Chung, W. E. Ruther, J. E. Sanecki, and T. F. Kassner, "Grain-Boundary Microchemistry and Intergranular Cracking of Irradiated Austenitic Stainless Steels," in Proc. 6th Intl. Symp. on Environmental Degradation of Materials in Nuclear Power Systems - Water Reactors, R. E. Gold and E. P. Simonen, eds., The Minerals, Metals, and Materials Society, Warrendale, PA, 1993, pp. 511-519.

10. J. M. Cookson, D. L. Damcott, G. S. Was, and P. L. Anderson, "The Role of Microchemical and Microstructural Effects in the IASCC of High-Purity Austenitic Stainless Steels," ibid., pp. 573-580.

11. M. Kodama, J. Morisawa, S. Nishimura, K. Asano, S. Shima, and K. Nakata, "Stress Corrosion Cracking and Intergranular Corrosion of Austenitic Stainless Steels Irradiated at 323 K," J. Nucl. Mater., 212–215 (1994) 1509.

12. T. Tsukada and Y. Miwa, "Stress Corrosion Cracking of Neutron Irradiated Stainless Steels," in Proc. 7th Intl. Symp. on Environmental Degradation of Materials in Nuclear Power Systems - Water Reactors, G. Airey et al., eds., NACE International, Houston, 1995, pp. 1009–1018.

13. F. Garzarolli, P. Dewes, R. Hahn, and J. L. Nelson, "In-Reactor Testing of IASCC Resistant Stainless Steels," ibid., 1055–1065.

14. H. M. Chung, W. E. Ruther, J. E. Sanecki, A. G. Hins, N. J. Zaluzec, and T. F. Kassner, "Irradiation–Assisted Stress Corrosion Cracking of Austenitic Stainless Steels: Recent Progress and New Approaches," J. Nucl. Mater., 239 (1996) 61.

15. J. M. Cookson, G. S. Was, and P. L. Anderson, "Oxide-Induced Initiation of Stress Corrosion Cracking in Irradiated Stainless Steels," Corrosion 54 (1998) 299.

16. S. Kasahara, K. Nakata, K. Fukuya, S. Shima, A. J. Jacobs, G. P. Wozadlo, and S. Suzuki, "The Effects of Minor Elements on IASCC Susceptibility in Austenitic Stainless Steels Irradiated with Neutrons," in Proc. 6th Intl. Symp. on Environmental Degradation of Materials in Nuclear Power Systems - Water Reactors, R. E. Gold and E. P. Simonen, eds., The Minerals, Metals, and Materials Society, Warrendale, PA, 1993, pp. 615-623.

17. A. Jenssen and L. G. Ljungberg, "Irradiation Assisted Stress Corrosion Cracking - Postirradiation CERT Tests of Stainless Steels in a BWR Test Loop," in Proc. 7th Intl. Symp. on Environmental Degradation of Materials in Nuclear Power Systems - Water Reactors, G. Airey et al., eds., NACE International, Houston, 1995, 1043–1052.

18. G. Taguchi, in "Quality Engineering Using Robust Design," M. S. Phadke, ed., Prentice Hall, Engelwood Cliffs, NJ, 1989.

19. H. M. Chung, W. E. Ruther, and R. V. Strain, "Irradiation-Assisted Stress Corrosion Cracking of Model Austenitic Stainless Steels Irradiated in the Halden Reactor," NUREG/CR-5608, ANL-98-25, Argonne National Laboratory, March 1999.

20. T. Tsukada, Y. Miwa, and T. Kondo, "Effects of Minor Elements on IASCC of Type 316 Model Stainless Steels," in Proc. 7th Intl. Symp. on Environmental Degradation of Materials in Nuclear Power Systems - Water Reactors, G. Airey et al., eds., NACE International, Houston, 1995, pp. 1009–1018.

21. "Sulfide Inclusions in Steel," Proc. Intl. Symp., November 7-8, 1974, Port Chester, New York, J. J. de Barbadillo and E. Snape, eds., American Society of Metals, 1975.

22. H. M. Chung, J. E. Sanecki, and F. A. Garner, "Radiation–Induced Instability of MnS Precipitates and Its Possible Consequences on Irradiation–Induced Stress Corrosion Cracking of Austenitic Stainless Steels," in Effects of Radiation on Materials: 18th Intl. Symp., ASTM STP 1325, R. K. Nanstad, M. L. Hamilton, A. S. Kumar, and F. A. Garner, eds., American Society for Testing and Material, 1999, pp. 647-658.

23. P. L. Andresen and C. L. Briant, "Role of S, P, and N Segregation on Intergranular Environmental Cracking of Stainless Steels in High Temperature Water," in Proc. 3rd Intl. Symp. on Environmental Degradation of Materials in Nuclear Power Systems – Water Reactors, G. J. Theus and J. R. Weeks, eds., The Metallurgical Society, Warrendale, PA, 1988, pp. 371-381.

NRC FORM 335 (2-89) NRCM 1102, 3201, 3202

U. S. NUCLEAR REGULATORY COMMISSION

BIBLIOGRAPHIC DATA SHEET

(See instructions on the reverse)

1. REPORT NUMBER *(Assigned by NRC. Add Vol., Supp., Rev., and Addendum Numbers, if any.)*
NUREG/CR-6687
ANL-00/21

2. TITLE AND SUBTITLE
Irradiation-Assisted Stress Corrosion Cracking of Model Austenitic Stainless Steel Alloys

3. DATE REPORT PUBLISHED
MONTH: October
YEAR: 2000

4. FIN OR GRANT NUMBER
W6610

5. AUTHOR(S)
H. M. Chung, W. E. Ruther, R. V. Strain, and W. J. Shack

6. TYPE OF REPORT
Technical; Topical

7. PERIOD COVERED *(Inclusive Dates)*

8. PERFORMING ORGANIZATION – NAME AND ADDRESS *(If NRC, provide Division, Office or Region, U.S. Nuclear Regulatory Commission, and mailing address; if contractor, provide name and mailing address.)*
Argonne National Laboratory
9700 South Cass Avenue
Argonne, IL 60439

9. SPONSORING ORGANIZATION – NAME AND ADDRESS *(If NRC, type "Same as above": if contractor, provide NRC Division, Office or Region, U.S. Nuclear Regulatory Commission, and mailing address.)*
Division of Engineering Technology
Office of Nuclear Regulatory Research
U. S. Nuclear Regulatory Commission
Washington, DC 20555-0001

10. SUPPLEMENTARY NOTES
M. NcNeil, NRC Project Manager

11. ABSTRACT (200 words or less)

This report summarizes work performed on irradiation-assisted stress corrosion cracking (IASCC) of model austenitic stainless steels (SSs) that were irradiated in the Halden reactor in simulation of boiling water reactor core internal components. Slow-strain-rate tensile tests were conducted on 16 austenitic stainless steel alloys that were irradiated to a fluence of $\approx 3 \times 10^{20}$ n cm^{-2} (E > 1 MeV) and 23 alloys irradiated to $\approx 9 \times 10^{20}$ n cm^{-2}. Fractographic analysis by scanning electron microscopy was also conducted to determine susceptibility to IASCC as manifested by transgranular and intergranular fracture surface morphology. Susceptibility to IASCC was influenced by more than one alloying and impurity element in a complex manner. For commercial heats of Types 304 and 304L SS, a high concentration of S is detrimental and a sufficiently low concentration of S (i.e., <0.009 wt.%) is a necessary condition for good resistance to IASCC. An alloy containing a high concentration of ≈21 wt.% Cr exhibited excellent resistance to IASCC, despite a high S content, indicating that Cr atoms in high concentration play a major role in suppressing susceptibility to IASCC. After irradiation, the degree of increase in yield strength was significantly lower for alloys that contain >0.9 wt.% Si than for alloys that contain <0.8 wt.% Si, indicating that the nature of hardening centers and the degree of irradiation hardening are significantly influenced by the Si content of the alloy. Similar influence was not observed for C and N. Results also indicate that a Si content between ≈0.8 and ≈1.5 wt.% is beneficial in delaying the onset of or suppressing the susceptibility to IASCC. Some alloys exhibited low uniform elongation and poor work-hardening capability in water after irradiation to $\approx 0.9 \times 10^{21}$ n·cm^{-2}, although the fracture surface morphology was mostly ductile. Such alloys contained unusually high concentrations of O or unusually low concentrations of Si or both.

12. KEY WORDS/DESCRIPTORS *(List words or phrases that will assist researchers in locating this report.)*
Boiling water reactor
In-core water chemistry
Core internal components
Irradiation-assisted stress corrosion cracking
Types 304 and 316 stainless steel
Transgranular stress corrosion cracking
Intergranular stress corrosion cracking
Work-hardening capability
Tensile ductility
Silicon, sulfur, oxygen, chromium

13. AVAILABILITY STATEMENT
Unlimited

14. SECURITY CLASSIFICATION
(This Page)
Unclassified
(This Report)
Unclassified

15. NUMBER OF PAGES

16. PRICE

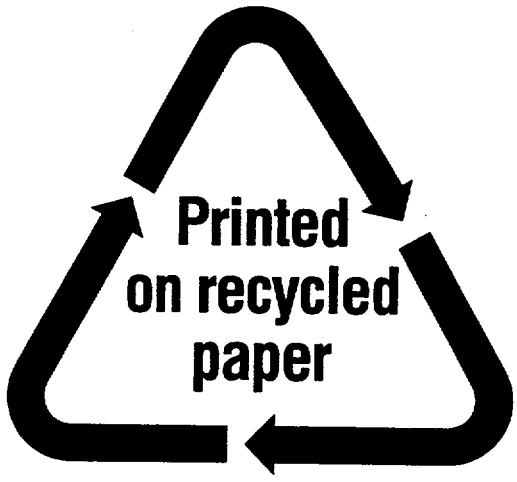

Federal Recycling Program

UNITED STATES
NUCLEAR REGULATORY COMMISSION
WASHINGTON, D.C. 20555-0001